Msh2-Msh3 interferes with DNA metabolism *in vivo*

Melisa Medina-Rivera[1#], Madhumita Sridharan[2], Jordan Becker[3], Samantha Phelps[1], Natalie A. Lamb[1&], Charanya Kumar[1%], Michaela Cornaire[1], Mark D. Sutton[1], Anja Bielinsky[3], Lata Balakrishnan[2], and Jennifer A. Surtees[1*]

[1]Department of Biochemistry, Jacobs School of Medicine and Biomedical Sciences, University at Buffalo

[2]Department of Biology, Indiana University Purdue University Indianapolis

[3]Department of Biochemistry, Molecular Biology and Biophysics, University of Minnesota

[#]Present address: Division of Nutritional Sciences, Cornell University

[&]Present address: UB Genomics and Bioinformatics Core

[%]Present address:

*Corresponding author: Jennifer A. Surtees, Tel: (716) 829-6083; Fax: (716) 829-2725: Email: jsurtees@buffalo.edu

ABSTRACT

Mismatch repair (MMR) is a highly conserved repair pathway essential to safeguard the genome from errors that occur during DNA replication. In *Saccharomyces cerevisiae*, two Msh complexes initiate MMR, either Msh2-Msh3 or Msh2-Msh6. These heterodimeric complexes recognize a number of DNA structures with varying affinities and play critical roles in DNA metabolism outside of post-replicative MMR; they contribute to genome stability through homologous recombination, double strand break repair (DSBR), and the DNA damage response.

In contrast to its role in promoting genome stability, Msh2-Msh3 is associated with genome instability through trinucleotide repeat (TNR) expansions. Msh2-Msh3's non-canonical activity in TNR expansions appears to be an unfortunate consequence of its intrinsic ability to bind to distinct DNA structures. Msh2-Msh3 binds to a wide range of DNA structures, including branched intermediates with 3' or 5' ss/ds DNA. Whereas the binding to 3' ssDNA tails leads to repair in a specialized form of DSBR called 3' non-homologous tail removal (3'NHTR), *in vitro* evidence suggests that Msh2-Msh3 binding to 5' flap structures interferes with the cleavage activity of the structure-specific endonuclease Rad27 (Fen1 in humans). The endonucleolytic function of Rad27 promotes 5' ssDNA flap processing during Okazaki fragment maturation and long-patch base excision repair (LP-BER). Here we show that elevated Msh2-Msh3 levels interfere with both DNA replication and BER *in vivo* in an expression and ATP-dependent manner, consistent with the hypothesis that protein abundance and ATPase activities in Msh3 are key drivers of Msh2-Msh3-mediated genomic instability.

INTRODUCTION

Mismatch repair (MMR) is a specialized DNA repair pathway known for its role in identifying and directing the correction of errors that evade the intrinsic fidelity mechanisms of the replication machinery, thereby increasing the fidelity of replication ~100–1000-fold (1-4). In *S. cerevisiae*, two heterodimer complexes initiate MMR with distinct but partially overlapping binding affinities (5,6). Msh2-Msh6 predominantly binds and directs the repair of single base mispairs (with the exception of C-C mismatches) and 1-2 nt insertion-deletion loops (IDLs) (6-10). Msh2-Msh3 binds and directs repair of some mispairs, including A-A, C-C and T-G (10-12), as well as both short and longer IDLs of up to 16nt in length (13-16). Following mismatch recognition, MutL homologs (Mlh) Mlh1-Mlh3 and/or Mlh1-Pms1 (Pms2 in humans) is recruited by MSH-DNA complexes in an ATP-dependent manner. The endonuclease activity of Mlh homologs is directed to cleave the nascent strand distal to the mismatch, an activity that requires a Msh complex. Mlh1-Pms1 is also activated by proliferating cell nuclear antigen (PCNA) (17-19), while Mlh1-Mlh3 is not (20,21). Subsequently, factors from the replication machinery, Exo1 and replicative DNA polymerase delta (Pol δ), or epsilon (Pol ε) are recruited to remove the error and resynthesize the DNA to restore the structure of the double helix (22-24).

Msh2-Msh3 is a structure-specific DNA-binding protein that binds a variety of different DNA intermediates, with a preference for substrates with double-strand (ds)/single-strand (ss) DNA junction (13,14,25,26). This allows Msh2-Msh3 to initiate several pathways in DNA metabolism in addition to MMR. Msh2-Msh3 participates during 3' non-homologous tail removal (3'NHTR), a step that occurs in a sub-type of double-strand DNA break repair (27-30). During 3' NHTR, Msh2-Msh3 binds to ds/ssDNA junctions with 3' ssDNA non-homologous tails, stabilizing the intermediate and recruiting the structure-specific endonuclease Rad1-Rad10/Saw1, thereby promoting cleavage of the unannealed tails and allowing repair to proceed via DNA synthesis (27,28,31). Msh2-Msh3 also promotes heteroduplex rejection, preventing recombination between homeologous sequences (32,33). In this context Msh2-Msh3 binds IDL structures, similar to MMR, but recruits Sgs1 to unwind the D-loop. (34,35). Given these known functions, it is not surprising that loss of Msh2-Msh3 is associated with an increase in genomic instabilities that contribute to hereditary and sporadic cancers in humans (36-48). Notably, Msh2-Msh3 binding to triplet repeat sequence leads to genome instability; Msh2-Msh3 promotes the expansion of (*CNG*) tracts and likely other repeat sequences,(49-55) including in *S. cerevisiae* (26,56,57). Similarly, Msh2-Msh3 binding to B-DNA/Z-DNA junctions promotes mutation (58). Msh2-Msh3 ATPase activity is required to promote genome stability through MMR, 3' NHTR and heteroduplex rejection (33) and to promote genome instability through TNR expansions (33). Like MutS and Msh2-Msh6, Msh2-Msh3 contains two composite ATP-binding/hydrolysis sites with highly conserved Walker A and Walker B

adenosine nucleotide-binding sites that are essential for nucleotide binding and catalysis, respectively (59-62). In *S. cerevisiae*, amino acid substitutions of the Walker A (G796 in Msh3), predicted to prevent ATP binding, abolished MMR, yielding a mutator phenotype similar to *msh3Δ* (63). Several studies have demonstrated that while nucleotide binding and hydrolysis is essential for Msh2-Msh3 function *in vivo*, it is dispensable for mismatch binding (14,63-70). Notably, Msh2-Msh3 binding to different DNA structures alters the kinetics of Msh2-Msh3 ATP binding, hydrolysis and nucleotide turnover, which are thought to impact downstream steps such as Msh2-Msh3 turnover and recruitment of other protein factors, leading to genome stability or instability (14,25,26,60,70-72).

5' ssDNA flaps are generated in at least two well-known DNA metabolic pathways: DNA replication (Okazaki fragment maturation), and long-patch base excision repair (LP-BER) (**Figure 1**). In each pathway Polymerase (Pol) δ can be recruited for synthesis. As Pol δ extends the initiator primer, it eventually encounters the preceding DNA fragment. Pol δ proceeds with synthesis and by doing so it displaces the 5'-end of the downstream segment forming a single-stranded 5' flap structure (73-75). This intermediate is cleaved by endonuclease Rad27 (FEN1 in humans), leaving a nick that is sealed by DNA ligase Cdc9 (DNA Ligase 1 (Lig1) in humans). We previously demonstrated that Msh2-Msh3 binds 5' ssDNA flap structures, albeit with lower affinity than 3' ssDNA flaps (14) to form a specific complex that interacts with the ss/dsDNA junction (26). We demonstrated that Msh2-Msh3 competes with both Rad27 and Lig1 for binding to DNA substrates. This resulted in inhibition of Rad27 endonuclease activity, ligation and a significant reduction of Okazaki fragment processing *in vitro* (26). Given that 5' flap processing is an essential step in DNA metabolism *in vivo*, uncontrolled binding of Msh2-Msh3 to 5' flap intermediates poses a potential risk for normal DNA metabolism.

Here we present evidence that elevated levels of Msh2-Msh3 interfere with DNA metabolism *in vivo*. Even low levels of Msh2-Msh3 overexpression resulted in sensitivity to the alkylating drug, methyl methanesulfonate (MMS), which generates lesions that are normally repaired via base excision repair (BER). Msh2-Msh3 overexpression also induced defects in cell cycle progression that may be a result of Okazaki fragment stress. Our results support a model in which elevated levels of Msh2-Msh3 interfere with normal DNA metabolism, not simply by binding DNA substrates, but by engaging in aberrant MMR in an ATP binding-dependent manner. Furthermore, they suggest that tight regulation of the Msh2-Msh3 expression levels is important *in vivo* to prevent interference with both DNA synthesis and the processing of a variety of DNA structures.

MATERIALS AND METHODS

Plasmids and Yeast Strains

To generate low copy and high copy plasmids expressing *MSH3* a *Sac*II-*Pst*I fragment from pEAI215 (71), which includes DNA sequence from ~ 1 kb upstream of *MSH3* to ~ 500 bp downstream of *MSH3* from its endogenous chromosomal location, was ligated into pRS423 (76) digested with *Sac*II and *Pst*I to generate pSP1. This is a high copy 2μ plasmid with a *LEU2* marker. From this plasmid, a *Sac*II-*Sal*I fragment was excised, containing the entire *MSH3* sequence from pEAI215, and ligated into pRS424 (76) and pRS414 (77) digested with *Sac*II and *Sal*I to generate pSP15 and pSP18, respectively. Both carry a *TRP1* marker; pSP15 is a 2μ plasmid while pSP18 is a single copy *ARS CEN* plasmid. Plasmids were transformed into a *msh3Δ* yeast strain background using the lithium acetate method (78).

Galactose-inducible overexpression plasmids of *MSH2* (pMMR8), *msh2G693D* (pEAE270), *MSH3* (pMMR20), *MSH6* (pEAE218), *msh3Y925A* (pCK94) and empty vector (pJAS104) were described previously (**Table S1)** (13,14,31,63,79)). To generate plasmids encoding galactose-inducible *msh3Y925A* and *msh3D870A* (pMME2 or pMME3), a *Bsu36I-MluI* fragment containing the *msh3* allele was sub-cloned into pMMR20 (13). Plasmids were co-transformed into a *msh3*Δ yeast strain background using the lithium acetate method (78). Strains used are described in **Table S2**.

RNA Isolation and Quantitative Real-Time PCR

Total RNA was isolated from cultured yeast cells utilizing the RNeasy Mini Kit from QIAGEN. As recommended by the manufacturer, residual DNA was removed by on-column DNase I digestion was carried out for 15 minutes. One μg of total RNA was reverse transcribed using a mix of oligo(dT) and random hexamer primers following manufacturer's instructions of the iScript™ cDNA synthesis kit (BioRad). Primers to detect endogenous transcript levels of *MSH2*, *MSH3*, *MSH6* and *PDA1* are described in **Table S3**. The RT-PCR was performed at 95 °C for 3 minutes, forty cycles of amplification consisting of denaturation at 95 °C for 15 s, annealing at 55 °C for 30 s, extension at 72 °C for 30 s, followed by melting curve analysis. Each RNA extraction was performed a minimum of three times. Each PCR included a standard curve with genomic DNA, and the levels of target transcripts were normalized to that of reference gene that encodes Pyruvate Dehydrogenase Alpha 1 (*PDA1*).

Galactose Inducible Overexpression

Cultures of a *msh3Δ* background (JSY1505 or JSY905) carrying both pMMR8 (*MSH2*) or pMMR8-derived (*msh2G693D*) and pMMR20 (*MSH3*) or pMMR20-derived (*msh3* alleles). (13) were grown to mid-log phase in synthetic complete (SC) medium in the presence of 2% lactate and 2% glycerol as carbon sources. Protein expression was induced by the addition of 2% galactose for 17 hours. Cells were harvested for flow cytometry, washed with sterile deionized water, fixed in 70% ethanol. They were stored

for up to 1 week at 4°C before flow cytometry analysis. Yeast cells for RNA extraction were washed with UltraPure™ DNase/RNase-Free Distilled Water (Invitrogen), harvested by centrifugation and resuspended in β-mercaptoethanol/Buffer RLT solution as described by RNeasy Mini Kit (QIAGEN) guidelines. Aliquots from each time point were snap-frozen in liquid nitrogen and stored at -80°C until ready for processing.

Methyl Methanesulfonate Survival Assays

For assays performed with high and low copy plasmids, cultures were grown to mid-log phase in SC(–Trp). Cells were diluted and plated on appropriate SC–Trp plates or SC–Trp plates containing 0.005, 0.01, 0.015, 0.0175 or 0.020% MMS. To avoid degradation of MMS and ensure consistent results, cells were plated within hours of pouring the plates. After incubation at 30°C for 4 days, percent survival was calculated as the ratio of the number of colonies that grew in presence of MMS relative to the no MMS control. Assays were repeated for a minimum of three times with at least two independent isolates.

For assays performed with overexpression strains, cultures were grown to mid-log phase in SC in the presence of lactate and glycerol as carbon sources. Protein expression was induced by as described above. Cells were diluted and plated into appropriate SC–Trp-Leu plates or SC–-Trp-Leu plates containing 0.005% MMS.

Cell Cycle Analysis

Yeast cells were washed with sodium citrate/EDTA solution (50mM sodium citrate and 1mM EDTA [pH 8.0]) and treated with 0.06mg RNase A (Invitrogen) at 50°C for 2 hours. This was followed with the addition of 0.25mg of Proteinase K (Sigma-Aldrich) and an incubation at 50°C for 2 hours. Cells were mixed with a sodium citrate/EDTA solution containing 1μM SYTOX® Green. Stained DNA was then analyzed for chromosomal content using a BD Fortessa Flow Cytometer at an excitation wavelength of 488nm. Data shown was analyzed using BD FACSDIVA™ software.

Canavanine Resistance Assays

Mutation rates were measured at the *CAN1* locus as previously described (80,81). Briefly, strains were grown on SC-Trp-Leu plates until colonies reach 2 mm in size. The carbon source in the plates was 2% glucose or 2% galactose for *MSH3* uninduced or induced, respectively. Colonies were then suspended in 100 μl of 1x TE (10 mM Tris-HCl, pH 7.4; 1 mM EDTA) and diluted 1:10,000. 20 μl of the undiluted colony suspension was plated on SC—Trp-Leu-Arg + Canavanine and 100 μl of the 10^{-4} dilution was plated on SC-Trp-Leu-Arg. Both permissive and selective plates contained 2% glucose as a carbon source. The plates were incubated at 30°C until colonies reached ~1 mm in size. Colonies were counted

and mutation rates and 95% confidence intervals were calculated though FluCalc fluctuation analysis software (82). Assays were performed on multiple, independent isolates for each genotype on separate days.

ATPase Assays

Hydrolysis of ATP was monitored using a coupled spectrophotometric assay as described previously (70,83). In this assay, the conversion of ATP to ADP and P_i is linked to the oxidation of NADH to NAD^+ and is monitored as a decrease in absorbance at 340 nm. Assays were performed at 30 °C and monitored using a Varian, Cary-50 Bio UV–vis spectrophotometer. The reactions contained 20 mM Tris–acetate (pH 7.5), 0.3 mM NADH, 5 mM PEP, 20 U/mL pyruvate kinase, 20 U/mL lactate dehydrogenase, 2 mM magnesium acetate, DNA (250 nM) and Msh2–Msh3 (50 nM) and up to 2.5 mM ATP. Msh2-Msh3 was pre-bound to DNA, followed by the addition of ATP in small increments. Approximately 80 data points were fit to a linear curve. The rate of ATP hydrolysis at each ATP concentration was calculated by multiplying the slope of the line by 159 (the change in absorbance of NADH per unit time).(83)

DNA Substrates

Oligonucleotides were synthesized by Integrated DNA Technologies (IDT, Coralville, IA) or Midland Certified Reagents Company (TX). Radiolabeled isotope was purchased from Perkin Elmer Life Sciences. Synthetic oligonucleotides were labeled with [γ ^{32}P]-ATP and T4 polynucleotide kinase (New England Biolabs) at their 5' end, as previously described (84). Following gel purification, substrate annealing was performed in a 1:2:4 ratio (labeled oligonucleotide: template: second oligonucleotide), as previously described (84). The oligonucleotides used in this study are listed in **Table S4**.

Protein purification

S. cerevisiae Msh2-Msh3 (70) and Pol δ (85) were expressed and purified as previously described.

Pol δ Strand Extension Assay

Two DNA substrates were used in the strand extension assays: the synthesis substrate and strand displacement substrate. The synthesis substrate was created by annealing 5' ^{32}P-labeled 44mer to 110nt template sequence in a 1:2 ratio respectively. The strand displacement substrate was created by annealing a 5' ^{32}P-labeled 44nt upstream primer to a110nt template containing a 60nt downstream primer in a 1:2:4 ratio. Five nM of the synthesis substrate was incubated with Pol δ (75nM with the synthesis substrate and 150nM for the strand displacement substrate) and increasing concentrations of Msh2-Msh3 (50nM, 100nM, 250nM) for 30 minutes at 30°C. Reactions were performed in 20µL volume in

reaction buffer containing 50Mm Tris-HCl pH 8.0; 2mM DTT, 2µg/mL bovine serum albumin, 8mM $MgCl_2$, 1mM ATP, 0.1mM dNTPs, 25nM NaCl. Reactions were terminated using 2X termination dye containing 90% formamide (v/v), 10 mM EDTA, with 0.01% bromophenol blue and xylene cyanole. Samples were then resolved on a 12% polyacrylamide gel containing 7M urea. Products were analyzed by a PhosphorImager (Typhoon 9500) and quantified using ImageQuant version 5.2 (Molecular Dynamics). All experiments were done at least in triplicate. Representative gels are shown.

Detection of PCNA Modification by Western Blot

Total proteins from yeast strains overexpressing Msh2-Msh3 were TCA precipitated as described in (86,87). The protein was analyzed by Western blot with an anti-PCNA antibody as described in (86,87).

RESULTS

Characterization of *MSH3* expression levels

Previous work demonstrated that Msh2-Msh3 binding to 5' flap substrates interferes with the processing of this intermediate by Rad27 and Cdc9 *in vitro*, likely through competition with Rad27 for binding the DNA intermediate (26). Since this intermediate occurs in multiple DNA metabolic pathways, such as long-patch BER and lagging strand synthesis, we were intrigued by the possibility that Msh2-Msh3 might interfere in these processes *in vivo,* potentially leading to genome instability and replication stress. Notably, altered levels of Msh2-Msh3 are a key driver of genome instability via TNR expansions in eukaryotes (88-91). Based on these results we set out to test the hypothesis that Msh2-Msh3 levels are a driver of genomic instability via 5' flap DNA intermediates.

To address the above hypothesis, we established a series of plasmids to express *MSH3* at different levels. First, we generated a single copy *ARS CEN* plasmid (pSP18, low copy [LC]) carrying *MSH3* under the control of its endogenous promoter. Second, we constructed a 2µ plasmid (pSP15, high copy [HC]) carrying *MSH3* under the control of its endogenous promoter. Finally, *MSH2* and *MSH3* were co-overexpressed in a *msh3Δ* background strain; *MSH2* (pMMR8) expression was under the control of the constitutive *ADC1* promoter, and *MSH3* (pMMR20) was expressed under the control of an inducible *GAL-PGK* promoter (13).

We performed quantitative RT-PCR (qRT-PCR) analysis to assess *MSH3* expression levels. The endogenous Msh3 protein levels and Msh3 levels in *msh3Δ* cells bearing a *MSH3* LC plasmid were too low to be reliably detectable by Western blot (11,63,92). RNA was extracted from wild-type and *msh3Δ* background strains in the presence or absence of the LC or HC *MSH3* plasmids, or both the *MSH2*

(pMMR8) and *MSH3* (pMMR20) plasmids. For co-overexpression experiments, sample aliquots were taken at different time points following induction with galactose to extract the RNA.

Consistent with low endogenous Msh3 protein levels, we observed endogenous *MSH3* mRNA levels to be six times lower than *MSH2* expression levels (**Figure 2A**). To increase expression levels, we transformed either a LC or HC plasmid, carrying *MSH3* under the control of its endogenous promoter, into the *msh3Δ* strain. The *MSH3* mRNA levels were four and sixty-four times higher than *MSH3* endogenous levels when expressed from the LC and HC plasmids, respectively (**Figure 2B**). To determine if upregulation of *MSH3* transcript levels influences the expression of *MSH2* or *MSH6*, we compared mRNA levels in the presence of the *MSH3* HC and LC plasmids; no significant differences were observed (**Figure 2B**).

To increase the expression levels further, a *msh3Δ* strain was co-transformed with a plasmid-borne copy of *MSH2,* expressed constitutively and at elevated levels, and a second plasmid bearing either a galactose-inducible copy of *MSH3* or an empty vector control. Galactose was added at mid-log phase to induce the overexpression of *MSH3.* Aliquots of several time points (0, 7, 14 and 17 hours after induction) were collected for qRT-PCR analysis. Prior to induction, we observed an increase in *MSH3* mRNA of approximately ~2,300-fold over *MSH3* endogenous levels (**Figure 2C**), indicating read-through transcription in the absence of galactose. As a control, *msh3Δ* co-expressing *MSH2* and the empty vector control derived from pMMR20 (pJAS104), expressed no *MSH3* mRNA (**Figure S1**). Upon induction by galactose for 17 h, *MSH3* expression levels increased to ~14-fold compared to the 0 h time point, or up to ~32,000 time higher than the endogenous levels of *MSH3* mRNA (**Figure 2C**). We previously demonstrated detectable Msh3 levels following induction and similar protein levels with point mutations tested (63). Other studies in human cell lines demonstrated that *MSH3* overexpression resulted in a strong Msh2-Msh6-specific mutator phenotype, presumably because excess Msh3 competed with Msh6 for interactions with Msh2 (90,93). To functionally test *MSH3* overexpression in yeast, we performed canavanine resistance assays, a Msh2-Msh6-specific mutator assay following co-overexpression of *MSH3* (**Table 1**). *MSH3* increased the mutation rates ~ 9 times, similar to the elevated mutation rate in *msh6Δ*.

Overexpression of Msh2-Msh3 leads to MMS sensitivity

The monofunctional alkylation agent MMS methylates DNA on the N^7-deoxyguanine and N^3-deoxyadenine (94), a lesion typically repaired by the BER pathway. Given the potential of Msh2-Msh3 to interfere with 5' flap processing we tested whether overexpression of *MSH3* or the co-expression of *MSH2* and *MSH3* sensitized the cells to MMS treatment, presumably by compromising LP-BER. *msh3Δ* yeast cells carrying a *MSH3* cloned into either a low copy number (*MSH3-LC*) or a high copy number

(*MSH3-HC*) plasmid were grown to mid-log phase, serial diluted and exposed to agar plates with or without MMS. At 0.015, 0.0175 or 0.02% of MMS concentration, both sets of transformants exhibited mild but significant sensitivity to MMS compared to controls (**Figure 3A**). When *MSH2* and *MSH3* were co-overexpressed, yeast cells exhibited even greater sensitivity to 0.005% MMS compared to overexpression of *MSH2* alone (**Figure 3B**). With higher *MSH3* overexpression, cells were sensitive to much lower MMS concentrations, consistent with a correlation between Msh3 levels and MMS sensitivity. This indicates that excess Msh2-Msh3 interferes with LP-BER.

Overexpression of Msh2-Msh3 interferes with cell cycle progression

Okazaki fragment maturation requires a 5' displaced flap processing step, interference with this process is associated with delays in cell cycle progression (87,95-99). To determine whether Msh2-Msh3 has the potential to interfere with cell cycle progression during Okazaki fragment maturation, we assessed cell cycle progression *via* flow cytometry in cells overexpressing *MSH2* and *MSH3*. When *MSH2* and *MSH3* were co-overexpressed, the effect on cell cycle progression was more dramatic and resulted in an accumulation of cells in S phase. Fourteen hours after induction with galactose, with a ~9-fold increase of *MSH3* mRNA levels compared to no induction (**Figure 2C**), we observed cell cycle progression defects, with an apparent accumulation of cells in early S phase (**Figure 4**). To quantify the populations in G1, S or G2/M phase cell cycle profiles were gated for the first collection point and kept constant throughout all time points collected (see **Figure S2**). When quantified, the percentage of cells in both G1 (1 DNA content, C1) and G2/M (2 DNA content, C2) phase decreased when *MSH2* and *MSH3* were overexpressed (compare time points 14 and 17.5 hours, **Figure 4A**). This observation is indicative of an accumulation of cells in S-phase, a phenotype that is associated with slow fork progression and/or DNA damage (100-102) (**Figure 4B, C**). Consistent with this observation, we observed ~ 2-fold increase in the number of cells in S phase with *MSH2 MSH3* overexpression. As a control, we co-overexpressed *MSH2* and *MSH6* (**Figure 5A**), which did not result in an accumulation of cells in S-phase. Similarly, overexpression of MSH2 alone was not sufficient to induce the cell cycle defect. These data suggest that overexpression of Msh2-Msh3, but not Msh2-Msh6, interferes with normal DNA metabolism. Our previous *in vitro* experiments indicated that Msh2-Msh3 out-competes Rad27 for binding to the ds/ssDNA junctions at 5' flaps (26). If Msh2-Msh3 outcompetes Rad27 *in vivo*, *MSH2 MSH3* overexpression could make the cells functionally *RAD27* null. Notably, the cell cycle profile of cells co-overexpressing *MSH2 MSH3* resembled that of *rad27Δ* at elevated temperature (98).

***MSH3* overexpression enhances PCNA post-translational modification**

Previous studies have shown that interference with Okazaki fragment processing leads to the cell cycle delays and DNA damage responses (86,87,98), signaling cascades that are mediated in part by post-translational modifications in PCNA (**Figure 6**). We examined whether overexpression of *MSH3* or *msh3* alleles could trigger a DNA damage response via post-transcriptional modification of PCNA. Following *MSH3* or *msh3G796A* or *msh3Y925A* overexpression, HA-tagged PCNA was immunoprecipitated from cell lysates and analyzed by western blot (86,87). When *MSH3* was overexpressed, a PCNA-specific band was observed near the bottom of the gel, consistent with the size of the unmodified PCNA (~29 kDa). In addition, a PCNA band with slower mobility was observed just below 49 kDa, consistent with a modified form of the protein subunits (**Figure 6**). This modified PCNA band was enhanced in the presence of *MSH3* overexpression compared to the empty vector (compare lanes 1 and 2, **Figure 6**).

Based on these data, one possibility was that *in vivo*, excess Msh2-Msh3 binding to 5' flaps sterically interfered with Okazaki fragment maturation. Alternatively, Msh2-Msh3 bound to 5' ssDNA flaps could promote aberrant Msh2-Msh3 activity that contributed to a signaling cascade leading to genome instability, similar to what is thought to occur in the presence of TNR structures (33).

msh3 alleles that disrupt ATP-binding and hydrolysis activities suppress disruption of cell cycle progression when overexpressed

To distinguish between these possibilities, we tested the effect of overexpression of *msh2* or *msh3* mutations on cell cycle progression. ATP plays essential roles in the function and regulation of Msh2-Msh3 but is not required for DNA binding (13,14,63,70,103). Therefore, if Msh2-Msh3 is simply binding to DNA structures and blocking Rad27, ATP binding and/or hydrolysis should be dispensable for inducing the cell cycle defect. In contrast, functional ATPase activity may be essential, as has been observed in TNR expansions (88,89). To test these possibilities, we monitored cell cycle progression while co-overexpressing *MSH2* and either *msh3G796A* or *msh3D870A* (63,88). These mutations disrupt the highly conserved Walker A motif (Msh3G796), which mediates ATP binding, or the Walker B motif (Msh3D870), which mediates ATP hydrolysis (60,63). Notably, cell cycle defects were abrogated when either one of these *msh3* alleles was overexpressed (**Figure 5B**). Similarly, disruption of the Msh2 Walker A motif, msh2G693D-Msh3, suppressed the cell cycle defects when overexpressed (**Figure 5C**), indicating the ATP binding to both Msh2 and Msh3 is required to disrupt cell cycle progression, likely via replication stress.

To determine whether normal regulation of ATP binding/hydrolysis was required to disrupt cell cycle progression, we overexpressed *msh3Y925A,* a separation-of-function allele that is defective in MMR, but functional in 3'NHTR (63). Based on the human Msh2-Msh3 crystal structure, Y925 is predicted

to regulate nucleotide occupancy of the nucleotide-binding pocket by pushing a conserved phenylalanine (F940) into the nucleotide-binding pocket (60). *In vitro* Msh2-msh3Y925A retains ATP hydrolysis activity but the kinetics of hydrolysis are significantly altered, indicating a defect in regulation of ATP binding, ATP hydrolysis and/or nucleotide turnover (**Figure S3**). When overexpressed, the *msh3Y925A* allele conferred cell cycle defects similar to the wild-type overexpression profile, consistent with the hypothesis that ATP binding/hydrolysis by Msh2-Msh3 is required for imposing cell cycle defects. However, regulation of this activity is apparently less important, as described for 3' NHTR (63). Combined, these data indicated that Msh2-Msh3 DNA-binding alone is not sufficient for the disruption of cell cycle progression.

The Walker A and Walker B mutations also abrogated modification of PCNA. Notably, co-overexpression of *MSH2 msh3Y925A* did promote PCNA modification, indicating that even misregulated ATPase activity was sufficient for this effect. These observations suggest that the cell cycle defect and PCNA modification are related and that an active Msh2-Msh3-mediated pathway promotes both phenotypes.

Notably, the modified PCNA band was not enhanced in the presence of *msh3G796A* overexpression, which disrupts the Walker A motif and therefore ATP binding (**Figure 6**). This correlates with the failure of this allele to perturb cell cycle progression (**Figure 5B**). In contrast, overexpression of *msh3Y925A*, which retains ATPase activity, led to PCNA modification that is indistinguishable from that in the presence of *MSH3* overexpression, again correlating with the cell cycle progression phenotype. These observations indicate that overexpression of the ATPase proficient Msh2-Msh3 alters cell-cycle progression and induces posttranslational modification of PCNA that might indicate replication stress and/or activation of a DNA damage response.

Downstream steps in MMR are required for cell cycle progression defects when *MSH3* is overexpressed

The observation that Msh2-Msh3 ATP binding and hydrolysis activities are required to observe defects in cell cycle progression and modification of PCNA indicated that downstream steps in a Msh2-Msh3-mediated pathway might also be required to observe these phenomena. In MMR, Msh2-Msh3 binding to specific DNA structures leads to the recruitment of Mlh complexes and activation of their latent endonuclease activity (20,21,104-108). Therefore, we tested the importance of *MLH1* for the cell cycle defect when *MSH2 MSH3* are co-overexpressed. We created a *mlh1Δ* strain, eliminating all three Mlh complexes, Mlh1-Pms1, Mlh1-Mlh2 and Mlh1-Mlh3. Upon induction of Msh2-Msh3 overexpression, the cell cycle profile in the *mlh1Δ* background largely resembles that in the presence of the empty vector (**Figure 5D**). However, overexpression of Msh2-Msh3 in absence of Mlh1 resulted in a peak to the left of

normal G1 (sub-G1). The sub-G1 peak is presumably the result of cells having reduced or lost DNA content during the cell cycle and is often associated apoptosis (100-102). These results indicate that Mlh complexes are required to observe the defects in cell cycle progression in the presence of *MSH3* overexpression. This observation suggests that one or more Mlh complexes contribute to Msh2-Msh3-mediated replication stress that disrupts the cell cycle.

Msh2-Msh3 modulates DNA Polymerase δ synthesis activity *in vitro*

We previously demonstrated that Msh2-Msh3 interferes with Rad27 and Lig1 activity when allowed to bind the relevant DNA substrates. Since Msh2-Msh3 binds has been shown to bind to ss-dsDNA junctions, we considered the possibility that Msh2-Msh3 interacting with different DNA structures might also impact DNA polymerase activity. As Pol δ is likely recruited in both Okazaki fragment processing and LP-BER, we tested Msh2-Msh3's effect on Pol δ activity *in vitro*. First, we assessed the ability of Msh2-Msh3 to modulate Pol δ synthesis on simple primer-template substrate (synthesis substrate). Titration of Msh2-Msh3 into a primer extension reaction inhibited synthesis by Pol δ (**Figure 7A**). We observed similar inhibition on the strand displacement substrate (observe substrate retention in lanes containing Msh2-Msh3). However, in contrast to synthesis inhibition, we also observed a stimulation in the strand displacement synthesis products on a small subset of substrates. (**Figure 7B**). We compared Msh2-Msh3 substrate binding efficiency on both substrates and found Msh2-Msh3 to bind efficiently to both substrates, albeit with lower affinity on the strand displacement substrate compared to the synthesis substrate (compare lane 3 to 6, **Figure 7A, right panel)**. These results indicated that Msh2-Msh3 can modify DNA metabolism pathways in a DNA structure-dependent manner, with variable impacts on genome stability.

DISCUSSION

Msh2-Msh3 has been shown to bind to a wide range of DNA structures, in both the yeast and human systems,(13,14,25,26,60,109,110) In this study, we demonstrated that Msh2-Msh3 has the potential to interfere with DNA metabolism pathways that involve 5' ssDNA flap intermediates *in vivo*. Even low levels of *MSH3* overexpression increased MMS sensitivity and compromised cell cycle progression through S phase. This effect was not simply due to Msh2-Msh3 binding to the DNA structure, but rather required downstream steps, including ATPase activity and MLH complexes. *MSH3* overexpression appeared to trigger a DNA damage response, leading to modification of PCNA.

Maintaining the "right" amount of Msh2-Msh3 is important for genome stability

Previous studies have measured relative levels of Msh2, Msh3 and Msh6 via mass spectrometry (111) or quantitative immunoblotting (112) and have observed an excess of Msh2 and Msh6 relative to Msh3. One semi-quantitative study using myc-tagged Msh proteins observed apparently similar levels of Msh3 and Msh6 (113). In this study, we assessed the transcript levels of untagged, endogenous *MSH2, MSH6,* and *MSH3* by qRT-PCR. Our results indicate that a wild-type yeast strain has a relative endogenous mRNA expression level of Msh6≅Msh2>Msh3. Approximately equal levels of Msh2 and Msh6 was consistent with our previous quantitative immunoblotting results (114). An imbalance in this distribution, by overexpressing Msh3, was previously linked with strong mutator phenotypes in human cells (90,93), presumably caused by a reduction in the formation of Msh2-Msh6 protein complexes. Consistent with this, when we overexpressed MSH3 alone, we observed an increase in canavanine resistance, which primarily measures Msh2-Msh6 activity. When we co-overexpressed *MSH2* and *MSH3* in budding yeast, we observed additional genomic instability phenotypes that included sensitivity to alkylating DNA damage (**Figure 3**), cell cycle delays (**Figures 4, 5**) and an enhancement of post-translational modified PCNA (**Figure 6**). Our results suggest that controlling the abundance of Msh3 is a mechanism by which a cell limits Msh2-Msh3 interactions with specific DNA structures, including 5' ssDNA flaps, that could promote genome instability. A similar correlation between Msh3 levels and TNR expansions was previously observed in a mouse model (89) and human cell lines (88). We predict that both the absolute levels of Msh2-Msh3 and the relative levels of Msh2-Msh3 versus Msh2-Msh6 are important to maintain the "right" balance of MMR activities in different cell and genomic contexts. Altered Msh2-Msh3 expression, up or down, can be deleterious. Downregulation of Msh2-Msh3 is linked to tumorigenesis and cancer (36,45,115), while an upregulation of Msh2-Msh3 is associated with microsatellite instabilities that promote TNR expansions (88,89). At the same time, Msh complexes are differentially expressed among organisms and tissues (89,93,115-117). For instance, analysis of Msh complexes abundance in actively proliferating murine tissues (including testis, spleen, and thymus) showed a higher expression of Msh6, but no Msh3 (116). In the same study, low proliferative tissues such as muscle, heart, and brain showed higher *MSH3* expression levels (116). These differences suggest that proliferating cells produce enough Msh2-Msh3 to participate in genome stability processes (*e.g.* MMR and 3'NHTR) but keep Msh3 in relatively low levels, when compared with Msh2 and Msh6, to prevent aberrant DNA metabolic processes.

An MMR-like response is required for Msh2-Msh3-mediated cell cycle genomic instabilities

The *in* vivo effects of elevated MSH3 or *MSH2 MSH3* expression suggested a simple model in which Msh2-Msh3 recognized and bound 5' ssDNA flap structures, as previously demonstrated *in vitro*,

(14,26) thereby blocking Rad27 activity *in vivo*. This would explain the MMS sensitivity, the defect in cell cycle progression through S phase and even modification of PCNA. However, two key sets of observations with mutations in several MMR components were inconsistent with this model and indicated an active, Msh2-Msh3-mediated MMR-like response. This is reminiscent of current models for the role of Msh2-Msh3 in promoting TNR expansions (33).

First, Msh2-Msh3-mediated S phase slow-down and modification of PCNA required ATPase activity. We and others have previously demonstrated that Msh2-Msh3 DNA-binding does not require ATP (13,14,25,72). In fact, the presence of ATP promotes dissociation from DNA *in vitro* (14,25,72,110). Mutations in the Walker A motif of Msh2 or Msh3 or in the Walker B motif of Msh3 blocked Msh2-Msh3-mediated phenotypes. Therefore, DNA-binding alone is not sufficient to observe the adverse effects of *MSH3* overexpression. Notably, the Walker A mutations have dominant negative effects *in vivo (*50,66); Msh2-msh3G693D inhibited ATP-dependent dissociation from DNA substrates *in vitro* (14). This further supports our prediction that Msh2-Msh3 is not simply binding to 5' ssDNA flaps and sterically hindering Rad27-mediated processing. In contrast, a mutation (*msh3Y925A*) that is predicted to alter the *regulation* of Msh2-Msh3 ATPase activity, did not block Msh2-Msh3-mediated interference with cell cycle progression. *msh3Y925A* also exhibited a dominant negative effect on MMR *in vivo* (63), indicating that this allele was able to interfere with MMR, but did not abrogate the *MSH3* overexpression phenotypes. We previously performed western blotting to assess mutant msh3 levels upon overexpression and found similar levels of Msh3, msh3G7976A and msh3Y925A (63), indicating that differential protein levels are unlikely to impact the phenotypes observed in this study.

Msh2-Msh3 or Msh2-msh3 complexes that retained ATPase activity also displayed an enhancement of a post-translational modified PCNA (**Figure 6**), consistent with elevated Msh2-Msh3 levels causing cell cycle stress in an ATP dependent manner.

Msh2-Msh3 ATPase activity is required for both Msh2-Msh3-mediated MMR and 3' NHTR (63,66,70), although there are differential requirements for the regulation of ATPase activity in these two pathways; *msh3Y925A* was defective in MMR but functional in 3' NHTR (63). Further, Msh2-Msh3 nucleotide binding, hydrolysis and turnover were differentially modulated by DNA substrates, consistent with differential DNA-dependent Msh2-Msh3 activities. Msh2-Msh3 ATPase activity is similarly required to promote TNR expansions; mutations in the Msh2 Walker A or Msh3 Walker B motif disrupted TNR expansions in mammalian systems (88,89). Msh2-Msh3 binding to TNR DNA substrates altered nucleotide (ADP and ATP) and hydrolysis (25,72,88). We hypothesize that Msh2-Msh3 binding to non-canonical DNA structures, such as TNR structures or 5' ssDNA flaps, alters the nucleotide binding/hydrolysis/turnover cycle and initiates an MMR-like response that is error-prone.

Second, we observed that loss of *MLH1*, which eliminates all three MLH complexes, prevented Msh2-Msh3-mediated interference of cell cycle progression. This suggests a model in which Msh2-msh3 mis-directs one or more MLH complexes when bound to 5' ssDNA flaps to interfere with Rad27-mediated DNA metabolic pathways. Notably, all three Mlh complexes play a role in Msh2-Msh3-mediated TNR expansion (118-123). Based on our data we suggest a model in which the endonuclease activity of Mlh complexes is misdirected by an altered nucleotide cycling of Msh2-Msh3 bound to a 5' ssDNA flap intermediate, similar to what has been proposed in TNR expansion studies.

A possible role of modified PCNA in Msh2-Msh3-mediated genome instability

PCNA can be modified by a variety of post-translational marks that expand the range of interactions with protein partners allowing to induction of signaling cascades for checkpoint activation, DNA repair or apoptosis (124). In eukaryotes, highly conserved lysine residues of PCNA are modified by ubiquitin and the small ubiquitin-related modifier SUMO in response to replication stress or DNA damage. Depending on the Lys residue and the type of post-translational modification that occurs a different DNA damage tolerance response is triggered. For instance, monoubiquitination of PCNA at Lys164 catalyzed by Rad6-Rad18 complex signals for the recruitment low fidelity translesion synthesis polymerases (such as Pol η, Rev1 and Pol ζ), which participate in an error-prone lesion bypass pathway (125-128). PCNA can be further poly-ubiquitinated by Ubc13-Mms2 and Rad5, which catalyze the formation of Lys63-linked ubiquitin chains on the Lys164 residue to yield recombination-based error-free outcome (127,129,130). Alternatively, PCNA can be SUMOylated on residues Lys127 and Lys164, by the Ubc9-Siz1 enzyme complex, to prevent unwanted recombination during S phase via the recruitment of the anti-recombinase Srs2 (127,131-133).

SUMOylated PCNA is also associated with the recruitment of Elg1 (134), a protein that substitutes for the large subunit in the RFC complex that is referred to as Elg1-RLC. In contrast to the clamp loader a function of RFC, Elg1-RLC is thought to facilitate the unloading of SUMOlyated PCNA and hence, performs an important function in PCNA recycling during lagging strand synthesis (134-137). Therefore, we reasoned that if Msh2-Msh3 is interfering cell cycle progression via 5' flap processing it might also be interrupting with the normal cycling of PCNA. Such events would result in an accumulation of SUMOylated PCNA at the replication fork, which would explain the enhancement of modified PCNA observed in **Figure 6**.

Model for *MSH2 MSH3* overexpression-mediated genome instability

In this study, we demonstrated that overexpression of Msh2-Msh3 complex in budding yeast can induce alkylation sensitivity (**Figure 3**), cell cycle progression delays (**Figures 4, 5**), and a putative PCNA-mediated DNA damage response (**Figure 6**). Our results are consistent with the idea that the upregulation of Msh2-Msh3 levels actively interferes with 5' flap processing *in vivo*. Both the Msh2-Msh3-mediated cell cycle defects and the PCNA modification required functional ATPase activity in the Msh2-Msh3 complex (**Figure 5, 6**). The cell cycle defects were abrogated in an *mlh1Δ* strain backgrounds (**Figure 5D**). These findings further support the idea that Msh2-Msh3 binding on its own is not sufficient to determine between genome stability or instability outcomes. These features are similar to the requirements of Msh2-Msh3 in promoting TNR expansions (25,26,72,138,139), possibly suggesting a common mechanism for promoting genomic instability.

Based on our results and the known functions of these proteins we propose the model: (*i*) Increased Msh2-Msh3 abundance increases the probability that Msh2-Msh3 will be available to bind ss/dsDNA junctions with 5' ssDNA flap intermediates that occur during Okazaki fragment maturation or long-patch BER. (*ii*) Binding a non-canonical DNA structure alters the coordination/cycle of nucleotide within the Msh2-Msh3 ATPase domain. (*iii*) Msh2-Msh3 recruits Mlh complexes leading to aberrant activation of the Mlh. Potentially the Mlh complex endonuclease activity is unregulated resulting in repeated rounds of nicking in an attempt to repair the DNA. Alternatively, Msh2-Msh3 bound to 5' ssDNA flap structures may misdirect Mlh endonuclease activity to the wrong strand, as has been demonstrated *in vitro* in the presence of TNR structures (140).

Msh2-Msh3 may also be directly affecting DNA synthesis in Okazaki fragment processing and/or LP-BER. We observed that Msh2-Msh3 either stimulated or inhibited DNA Pol δ activity *in vitro*, in a DNA substrate-dependent manner. In the presence of a simple primer-template substrate, Msh2-Msh3 inhibited complete, full-length synthesis. In contrast, Msh2-Msh3 enhanced the production of full-length products in the presence of a gapped substrate that required Pol δ strand displacement activity. These observations, coupled with differential affinity of Msh2-Msh3 for binding these substrates, predict a model in which Msh2-Msh3 binds and alters that conformation of the DNA structures to enhance or inhibit Pol δ activity. *In vivo*, Msh2-Msh3 could, when in sufficient quantities, similarly modulate Pol δ activity, altering the kinetics of DNA synthesis.

Table 1. Canavanine resistance mutation rates			
Genotype	**Carbon source**	**Rate of Canavanine Resistance [95% confidence intervals]**	**Change (Relative to glucose)**
WT	glucose	3.9×10^{-7} [$2.5 \times 10^{-7} – 5.5 \times 10^{-7}$]	1
WT	galactose	3.5 x 10-7 [$2.5 \times 10^{-7} – 4.5 \times 10^{-7}$]	0.9
WT + MSH3 O/E	glucose	7.9×10^{-7} [$6.5 \times 10^{-7} – 9.3 \times 10^{-7}$]	1
WT + MSH3 O/E	galactose	7.2×10^{-6} [$6.6 \times 10^{-6} – 7.9 \times 10^{-6}$]	9.1

ACKNOWLEDGEMENT: We are grateful for the support of the UB Confocal Microscope and Flow Cytometry Facility (CMFCF).

FUNDING: This work was supported by IMSD training grant (R25 GM095459) and diversity supplement (GM066094) to MMR, National Science Foundation (1929346) to LB, NIH grants R35GM141805 and R01GM134681 to AKB, NIH grant GM087459 and American Cancer Society Research Scholar Grant (RSG-14-2350-01) to JAS. JAS is also grateful for support from the University at Buffalo's Genome, Environment and Microbiome Community of Excellence.

Funding for open access charge: University at Buffalo's Genome, Environment and Microbiome Community of Excellence.

CONFLICT OF INTEREST

The authors declare they have no conflict of interest.

REFERENCES

1. Modrich, P. and Lahue, R. (1996) Mismatch repair in replication fidelity, genetic recombination, and cancer biology. *Annu Rev Biochem*, **65**, 101-133.
2. Iyer, R.R., Pluciennik, A., Burdett, V. and Modrich, P.L. (2006) DNA mismatch repair: functions and mechanisms. *Chem Rev*, **106**, 302-323.
3. McCulloch, S.D. and Kunkel, T.A. (2008) The fidelity of DNA synthesis by eukaryotic replicative and translesion synthesis polymerases. *Cell Res*, **18**, 148-161.
4. Ganai, R.A. and Johansson, E. (2016) DNA Replication-A Matter of Fidelity. *Mol Cell*, **62**, 745-755.
5. Acharya, S., Wilson, T., Gradia, S., Kane, M.F., Guerrette, S., Marsischky, G.T., Kolodner, R. and Fishel, R. (1996) hMSH2 forms specific mispair-binding complexes with hMSH3 and hMSH6. *Proc Natl Acad Sci U S A*, **93**, 13629-13634.
6. Marsischky, G.T., Filosi, N., Kane, M.F. and Kolodner, R. (1996) Redundancy of Saccharomyces cerevisiae MSH3 and MSH6 in MSH2-dependent mismatch repair. *Genes Dev*, **10**, 407-420.
7. Alani, E. (1996) The Saccharomyces cerevisiae Msh2 and Msh6 proteins form a complex that specifically binds to duplex oligonucleotides containing mismatched DNA base pairs. *Mol Cell Biol*, **16**, 5604-5615.
8. Iaccarino, I., Palombo, F., Drummond, J., Totty, N.F., Hsuan, J.J., Modrich, P. and Jiricny, J. (1996) MSH6, a Saccharomyces cerevisiae protein that binds to mismatches as a heterodimer with MSH2. *Curr Biol*, **6**, 484-486.
9. Marsischky, G.T. and Kolodner, R.D. (1999) Biochemical characterization of the interaction between the Saccharomyces cerevisiae MSH2-MSH6 complex and mispaired bases in DNA. *J Biol Chem*, **274**, 26668-26682.
10. Lamb, N.A., Bard, J.E., Loll-Krippleber, R., Brown, G.W. and Surtees, J.A. (2022) Complex mutation profiles in mismatch repair and ribonucleotide reductase mutants reveal novel repair substrate specificity of MutS homolog (MSH) complexes. *Genetics*, **221**.
11. Harrington, J.M. and Kolodner, R.D. (2007) Saccharomyces cerevisiae Msh2-Msh3 acts in repair of base-base mispairs. *Mol Cell Biol*, **27**, 6546-6554.
12. Srivatsan, A., Bowen, N. and Kolodner, R.D. (2014) Mispair-specific recruitment of the Mlh1-Pms1 complex identifies repair substrates of the Saccharomyces cerevisiae Msh2-Msh3 complex. *J Biol Chem*, **289**, 9352-9364.
13. Habraken, Y., Sung, P., Prakash, L. and Prakash, S. (1996) Binding of insertion/deletion DNA mismatches by the heterodimer of yeast mismatch repair proteins MSH2 and MSH3. *Curr Biol*, **6**, 1185-1187.
14. Surtees, J.A. and Alani, E. (2006) Mismatch repair factor MSH2-MSH3 binds and alters the conformation of branched DNA structures predicted to form during genetic recombination. *J Mol Biol*, **360**, 523-536.
15. Sia, E.A., Kokoska, R.J., Dominska, M., Greenwell, P. and Petes, T.D. (1997) Microsatellite instability in yeast: dependence on repeat unit size and DNA mismatch repair genes. *Mol Cell Biol*, **17**, 2851-2858.
16. Jensen, L.E., Jauert, P.A. and Kirkpatrick, D.T. (2005) The large loop repair and mismatch repair pathways of Saccharomyces cerevisiae act on distinct substrates during meiosis. *Genetics*, **170**, 1033-1043.

17. Plotz, G., Welsch, C., Giron-Monzon, L., Friedhoff, P., Albrecht, M., Piiper, A., Biondi, R.M., Lengauer, T., Zeuzem, S. and Raedle, J. (2006) Mutations in the MutSalpha interaction interface of MLH1 can abolish DNA mismatch repair. *Nucleic Acids Res*, **34**, 6574-6586.
18. Pluciennik, A., Dzantiev, L., Iyer, R.R., Constantin, N., Kadyrov, F.A. and Modrich, P. (2010) PCNA function in the activation and strand direction of MutLα endonuclease in mismatch repair. *Proceedings of the National Academy of Sciences*, **107**, 16066-16071.
19. Goellner, E.M., Smith, C.E., Campbell, C.S., Hombauer, H., Desai, A., Putnam, C.D. and Kolodner, R.D. (2014) PCNA and Msh2-Msh6 activate an Mlh1-Pms1 endonuclease pathway required for Exo1-independent mismatch repair. *Mol Cell*, **55**, 291-304.
20. Rogacheva, M.V., Manhart, C.M., Chen, C., Guarne, A., Surtees, J. and Alani, E. (2014) Mlh1-Mlh3, a meiotic crossover and DNA mismatch repair factor, is a Msh2-Msh3-stimulated endonuclease. *J Biol Chem*, **289**, 5664-5673.
21. Manhart, C.M., Ni, X., White, M.A., Ortega, J., Surtees, J.A. and Alani, E. (2017) The mismatch repair and meiotic recombination endonuclease Mlh1-Mlh3 is activated by polymer formation and can cleave DNA substrates in trans. *PLoS Biol*, **15**, e2001164.
22. Kunkel, T.A. and Erie, D.A. (2015) Eukaryotic Mismatch Repair in Relation to DNA Replication. *Annu Rev Genet*, **49**, 291-313.
23. Kunkel, T.A. and Erie, D.A. (2005) DNA mismatch repair. *Annu Rev Biochem*, **74**, 681-710.
24. Bowen, N. and Kolodner, R.D. (2017) Reconstitution of Saccharomyces cerevisiae DNA polymerase ε-dependent mismatch repair with purified proteins. *Proc Natl Acad Sci U S A*, **114**, 3607-3612.
25. Owen, B.A., Yang, Z., Lai, M., Gajec, M., Badger, J.D., 2nd, Hayes, J.J., Edelmann, W., Kucherlapati, R., Wilson, T.M. and McMurray, C.T. (2005) (CAG)(n)-hairpin DNA binds to Msh2-Msh3 and changes properties of mismatch recognition. *Nat Struct Mol Biol*, **12**, 663-670.
26. Kantartzis, A., Williams, G.M., Balakrishnan, L., Roberts, R.L., Surtees, J.A. and Bambara, R.A. (2012) Msh2-Msh3 interferes with Okazaki fragment processing to promote trinucleotide repeat expansions. *Cell Rep*, **2**, 216-222.
27. Li, F., Dong, J., Eichmiller, R., Holland, C., Minca, E., Prakash, R., Sung, P., Yong Shim, E., Surtees, J.A. and Eun Lee, S. (2013) Role of Saw1 in Rad1/Rad10 complex assembly at recombination intermediates in budding yeast. *Embo j*, **32**, 461-472.
28. Sugawara, N., Pâques, F., Colaiácovo, M. and Haber, J.E. (1997) Role of Saccharomyces cerevisiae Msh2 and Msh3 repair proteins in double-strand break-induced recombination. *Proc Natl Acad Sci U S A*, **94**, 9214-9219.
29. Evans, E., Sugawara, N., Haber, J.E. and Alani, E. (2000) The Saccharomyces cerevisiae Msh2 mismatch repair protein localizes to recombination intermediates in vivo. *Mol Cell*, **5**, 789-799.
30. Saparbaev, M., Prakash, L. and Prakash, S. (1996) Requirement of mismatch repair genes MSH2 and MSH3 in the RAD1-RAD10 pathway of mitotic recombination in Saccharomyces cerevisiae. *Genetics*, **142**, 727-736.
31. Eichmiller, R., Medina-Rivera, M., DeSanto, R., Minca, E., Kim, C., Holland, C., Seol, J.H., Schmit, M., Oramus, D., Smith, J. *et al.* (2018) Coordination of Rad1-Rad10 interactions with Msh2-Msh3, Saw1 and RPA is essential for functional 3' non-homologous tail removal. *Nucleic Acids Res*, **46**, 5075-5096.
32. Jiang, J., Bai, L., Surtees, J.A., Gemici, Z., Wang, M.D. and Alani, E. (2005) Detection of high-affinity and sliding clamp modes for MSH2-MSH6 by single-molecule unzipping force analysis. *Mol Cell*, **20**, 771-781.

33. Refsland, E.W. and Livingston, D.M. (2005) Interactions among DNA ligase I, the flap endonuclease and proliferating cell nuclear antigen in the expansion and contraction of CAG repeat tracts in yeast. *Genetics*, **171**, 923-934.
34. Sugawara, N., Goldfarb, T., Studamire, B., Alani, E. and Haber, J.E. (2004) Heteroduplex rejection during single-strand annealing requires Sgs1 helicase and mismatch repair proteins Msh2 and Msh6 but not Pms1. *Proc Natl Acad Sci U S A*, **101**, 9315-9320.
35. Chakraborty, U. and Alani, E. (2016) Understanding how mismatch repair proteins participate in the repair/anti-recombination decision. *FEMS Yeast Res*, **16**.
36. Edelmann, W., Umar, A., Yang, K., Heyer, J., Kucherlapati, M., Lia, M., Kneitz, B., Avdievich, E., Fan, K., Wong, E. *et al.* (2000) The DNA mismatch repair genes Msh3 and Msh6 cooperate in intestinal tumor suppression. *Cancer Res*, **60**, 803-807.
37. van Oers, J.M., Edwards, Y., Chahwan, R., Zhang, W., Smith, C., Pechuan, X., Schaetzlein, S., Jin, B., Wang, Y., Bergman, A. *et al.* (2014) The MutSβ complex is a modulator of p53-driven tumorigenesis through its functions in both DNA double-strand break repair and mismatch repair. *Oncogene*, **33**, 3939-3946.
38. Santos, L.S., Silva, S.N., Gil, O.M., Ferreira, T.C., Limbert, E. and Rueff, J. (2018) Mismatch repair single nucleotide polymorphisms and thyroid cancer susceptibility. *Oncol Lett*, **15**, 6715-6726.
39. Ashktorab, H., Azimi, H., Varma, S., Tavakoli, P., Nickerson, M.L. and Brim, H. (2017) Distinctive DNA mismatch repair and APC rare variants in African Americans with colorectal neoplasia. *Oncotarget*, **8**, 99966-99977.
40. Raskin, L., Guo, Y., Du, L., Clendenning, M., Rosty, C., Lindor, N.M., Gruber, S.B. and Buchanan, D.D. (2017) Targeted sequencing of established and candidate colorectal cancer genes in the Colon Cancer Family Registry Cohort. *Oncotarget*, **8**, 93450-93463.
41. Morak, M., Käsbauer, S., Kerscher, M., Laner, A., Nissen, A.M., Benet-Pagès, A., Schackert, H.K., Keller, G., Massdorf, T. and Holinski-Feder, E. (2017) Loss of MSH2 and MSH6 due to heterozygous germline defects in MSH3 and MSH6. *Fam Cancer*, **16**, 491-500.
42. Takahashi, M., Koi, M., Balaguer, F., Boland, C.R. and Goel, A. (2011) MSH3 mediates sensitization of colorectal cancer cells to cisplatin, oxaliplatin, and a poly(ADP-ribose) polymerase inhibitor. *J Biol Chem*, **286**, 12157-12165.
43. Park, J.M., Huang, S., Tougeron, D. and Sinicrope, F.A. (2013) MSH3 mismatch repair protein regulates sensitivity to cytotoxic drugs and a histone deacetylase inhibitor in human colon carcinoma cells. *PLoS One*, **8**, e65369.
44. Nogueira, G.A.S., Costa, E.F.D., Lopes-Aguiar, L., Lima, T.R.P., Visacri, M.B., Pincinato, E.C., Lourenço, G.J., Calonga, L., Mariano, F.V., Altemani, A. *et al.* (2018) Polymorphisms in DNA mismatch repair pathway genes predict toxicity and response to cisplatin chemoradiation in head and neck squamous cell carcinoma patients. *Oncotarget*, **9**, 29538-29547.
45. Miao, H.K., Chen, L.P., Cai, D.P., Kong, W.J., Xiao, L. and Lin, J. (2015) MSH3 rs26279 polymorphism increases cancer risk: a meta-analysis. *Int J Clin Exp Pathol*, **8**, 11060-11067.
46. Dietlein, F., Thelen, L., Jokic, M., Jachimowicz, R.D., Ivan, L., Knittel, G., Leeser, U., van Oers, J., Edelmann, W., Heukamp, L.C. *et al.* (2014) A functional cancer genomics screen identifies a druggable synthetic lethal interaction between MSH3 and PRKDC. *Cancer Discov*, **4**, 592-605.
47. Carethers, J.M. (2017) Microsatellite Instability Pathway and EMAST in Colorectal Cancer. *Curr Colorectal Cancer Rep*, **13**, 73-80.
48. Adam, R., Spier, I., Zhao, B., Kloth, M., Marquez, J., Hinrichsen, I., Kirfel, J., Tafazzoli, A., Horpaopan, S., Uhlhaas, S. *et al.* (2016) Exome Sequencing Identifies Biallelic MSH3 Germline

Mutations as a Recessive Subtype of Colorectal Adenomatous Polyposis. *Am J Hum Genet*, **99**, 337-351.
49. Iyer, R.R., Pluciennik, A., Napierala, M. and Wells, R.D. (2015) DNA triplet repeat expansion and mismatch repair. *Annu Rev Biochem*, **84**, 199-226.
50. Massey, T.H. and Jones, L. (2018) The central role of DNA damage and repair in CAG repeat diseases. *Dis Model Mech*, **11**.
51. Jones, L., Houlden, H. and Tabrizi, S.J. (2017) DNA repair in the trinucleotide repeat disorders. *Lancet Neurol*, **16**, 88-96.
52. Schmidt, M.H.M. and Pearson, C.E. (2016) Disease-associated repeat instability and mismatch repair. *DNA Repair (Amst)*, **38**, 117-126.
53. Usdin, K., House, N.C. and Freudenreich, C.H. (2015) Repeat instability during DNA repair: Insights from model systems. *Crit Rev Biochem Mol Biol*, **50**, 142-167.
54. Du, J., Campau, E., Soragni, E., Ku, S., Puckett, J.W., Dervan, P.B. and Gottesfeld, J.M. (2012) Role of mismatch repair enzymes in GAA·TTC triplet-repeat expansion in Friedreich ataxia induced pluripotent stem cells. *J Biol Chem*, **287**, 29861-29872.
55. McGinty, R.J. and Mirkin, S.M. (2018) Cis- and Trans-Modifiers of Repeat Expansions: Blending Model Systems with Human Genetics. *Trends Genet*, **34**, 448-465.
56. Williams, G.M. and Surtees, J.A. (2015) MSH3 Promotes Dynamic Behavior of Trinucleotide Repeat Tracts In Vivo. *Genetics*, **200**, 737-754.
57. Williams, G.M., Petrides, A.K., Balakrishnan, L. and Surtees, J.A. (2020) Tracking Expansions of Stable and Threshold Length Trinucleotide Repeat Tracts In Vivo and In Vitro Using Saccharomyces cerevisiae. *Methods Mol Biol*, **2056**, 25-68.
58. McKinney, J.A., Wang, G., Mukherjee, A., Christensen, L., Subramanian, S.H.S., Zhao, J. and Vasquez, K.M. (2020) Distinct DNA repair pathways cause genomic instability at alternative DNA structures. *Nat Commun*, **11**, 236.
59. Obmolova, G., Ban, C., Hsieh, P. and Yang, W. (2000) Crystal structures of mismatch repair protein MutS and its complex with a substrate DNA. *Nature*, **407**, 703-710.
60. Gupta, S., Gellert, M. and Yang, W. (2011) Mechanism of mismatch recognition revealed by human MutSβ bound to unpaired DNA loops. *Nat Struct Mol Biol*, **19**, 72-78.
61. Lamers, M.H., Perrakis, A., Enzlin, J.H., Winterwerp, H.H., de Wind, N. and Sixma, T.K. (2000) The crystal structure of DNA mismatch repair protein MutS binding to a G x T mismatch. *Nature*, **407**, 711-717.
62. Warren, J.J., Pohlhaus, T.J., Changela, A., Iyer, R.R., Modrich, P.L. and Beese, L.S. (2007) Structure of the human MutSalpha DNA lesion recognition complex. *Mol Cell*, **26**, 579-592.
63. Kumar, C., Williams, G.M., Havens, B., Dinicola, M.K. and Surtees, J.A. (2013) Distinct requirements within the Msh3 nucleotide binding pocket for mismatch and double-strand break repair. *J Mol Biol*, **425**, 1881-1898.
64. Alani, E., Sokolsky, T., Studamire, B., Miret, J.J. and Lahue, R.S. (1997) Genetic and biochemical analysis of Msh2p-Msh6p: role of ATP hydrolysis and Msh2p-Msh6p subunit interactions in mismatch base pair recognition. *Mol Cell Biol*, **17**, 2436-2447.
65. Iaccarino, I., Marra, G., Palombo, F. and Jiricny, J. (1998) hMSH2 and hMSH6 play distinct roles in mismatch binding and contribute differently to the ATPase activity of hMutSalpha. *Embo j*, **17**, 2677-2686.
66. Studamire, B., Quach, T. and Alani, E. (1998) Saccharomyces cerevisiae Msh2p and Msh6p ATPase activities are both required during mismatch repair. *Mol Cell Biol*, **18**, 7590-7601.

67. Au, K.G., Welsh, K. and Modrich, P. (1992) Initiation of methyl-directed mismatch repair. *J Biol Chem*, **267**, 12142-12148.
68. Drotschmann, K., Yang, W. and Kunkel, T.A. (2002) Evidence for sequential action of two ATPase active sites in yeast Msh2-Msh6. *DNA Repair (Amst)*, **1**, 743-753.
69. Acharya, S. and Patterson, K. (2010) Mutations in the conserved glycine and serine of the MutS ABC signature motif affect nucleotide exchange, kinetics of sliding clamp release of mismatch and mismatch repair. *Mutat Res*, **684**, 56-65.
70. Kumar, C., Eichmiller, R., Wang, B., Williams, G.M., Bianco, P.R. and Surtees, J.A. (2014) ATP binding and hydrolysis by Saccharomyces cerevisiae Msh2-Msh3 are differentially modulated by mismatch and double-strand break repair DNA substrates. *DNA Repair (Amst)*, **18**, 18-30.
71. Lee, S.D., Surtees, J.A. and Alani, E. (2007) Saccharomyces cerevisiae MSH2-MSH3 and MSH2-MSH6 complexes display distinct requirements for DNA binding domain I in mismatch recognition. *J Mol Biol*, **366**, 53-66.
72. Lang, W.H., Coats, J.E., Majka, J., Hura, G.L., Lin, Y., Rasnik, I. and McMurray, C.T. (2011) Conformational trapping of mismatch recognition complex MSH2/MSH3 on repair-resistant DNA loops. *Proc Natl Acad Sci U S A*, **108**, E837-844.
73. Bambara, R.A., Murante, R.S. and Henricksen, L.A. (1997) Enzymes and reactions at the eukaryotic DNA replication fork. *J Biol Chem*, **272**, 4647-4650.
74. Liu, Y., Zhang, H., Veeraraghavan, J., Bambara, R.A. and Freudenreich, C.H. (2004) Saccharomyces cerevisiae flap endonuclease 1 uses flap equilibration to maintain triplet repeat stability. *Mol Cell Biol*, **24**, 4049-4064.
75. Burgers, P.M. (2009) Polymerase dynamics at the eukaryotic DNA replication fork. *J Biol Chem*, **284**, 4041-4045.
76. Christianson, T.W., Sikorski, R.S., Dante, M., Shero, J.H. and Hieter, P. (1992) Multifunctional yeast high-copy-number shuttle vectors. *Gene*, **110**, 119-122.
77. Sikorski, R.S. and Hieter, P. (1989) A system of shuttle vectors and yeast host strains designed for efficient manipulation of DNA in Saccharomyces cerevisiae. *Genetics*, **122**, 19-27.
78. Gietz, D., St Jean, A., Woods, R.A. and Schiestl, R.H. (1992) Improved method for high efficiency transformation of intact yeast cells. *Nucleic Acids Res*, **20**, 1425.
79. Kijas, A.W., Studamire, B. and Alani, E. (2003) Msh2 separation of function mutations confer defects in the initiation steps of mismatch repair. *J Mol Biol*, **331**, 123-138.
80. Xu, X., Page, J.L., Surtees, J.A., Liu, H., Lagedrost, S., Lu, Y., Bronson, R., Alani, E., Nikitin, A.Y. and Weiss, R.S. (2008) Broad overexpression of ribonucleotide reductase genes in mice specifically induces lung neoplasms. *Cancer Res*, **68**, 2652-2660.
81. Lamb, N.A., Bard, J.E., Buck, M.J. and Surtees, J.A. (2021) A selection-based next generation sequencing approach to develop robust, genotype-specific mutation profiles in Saccharomyces cerevisiae. *G3 (Bethesda)*.
82. Radchenko, E.A., McGinty, R.J., Aksenova, A.Y., Neil, A.J. and Mirkin, S.M. (2018) Quantitative Analysis of the Rates for Repeat-Mediated Genome Instability in a Yeast Experimental System. *Methods Mol Biol*, **1672**, 421-438.
83. Bianco, P.R., Xu, C. and Chi, M. (2009) Type I restriction endonucleases are true catalytic enzymes. *Nucleic Acids Res*, **37**, 3377-3390.
84. Stewart, J.A., Campbell, J.L. and Bambara, R.A. (2006) Flap endonuclease disengages Dna2 helicase/nuclease from Okazaki fragment flaps. *J Biol Chem*, **281**, 38565-38572.

85. Langston, L.D. and O'Donnell, M. (2008) DNA polymerase delta is highly processive with proliferating cell nuclear antigen and undergoes collision release upon completing DNA. *J Biol Chem*, **283**, 29522-29531.
86. Das-Bradoo, S., Nguyen, H.D., Wood, J.L., Ricke, R.M., Haworth, J.C. and Bielinsky, A.K. (2010) Defects in DNA ligase I trigger PCNA ubiquitylation at Lys 107. *Nat Cell Biol*, **12**, 74-79; sup pp 71-20.
87. Nguyen, H.D., Becker, J., Thu, Y.M., Costanzo, M., Koch, E.N., Smith, S., Myung, K., Myers, C.L., Boone, C. and Bielinsky, A.K. (2013) Unligated Okazaki Fragments Induce PCNA Ubiquitination and a Requirement for Rad59-Dependent Replication Fork Progression. *PLoS One*, **8**, e66379.
88. Keogh, N., Chan, K.Y., Li, G.M. and Lahue, R.S. (2017) MutSβ abundance and Msh3 ATP hydrolysis activity are important drivers of CTG•CAG repeat expansions. *Nucleic Acids Res*, **45**, 10068-10078.
89. Tomé, S., Manley, K., Simard, J.P., Clark, G.W., Slean, M.M., Swami, M., Shelbourne, P.F., Tillier, E.R., Monckton, D.G., Messer, A. *et al.* (2013) MSH3 polymorphisms and protein levels affect CAG repeat instability in Huntington's disease mice. *PLoS Genet*, **9**, e1003280.
90. Drummond, J.T., Genschel, J., Wolf, E. and Modrich, P. (1997) DHFR/MSH3 amplification in methotrexate-resistant cells alters the hMutSalpha/hMutSbeta ratio and reduces the efficiency of base-base mismatch repair. *Proc Natl Acad Sci U S A*, **94**, 10144-10149.
91. Ioana, M., Angelescu, C., Burada, F., Mixich, F., Riza, A., Dumitrescu, T., Alexandru, D., Ciurea, T., Cruce, M. and Saftoiu, A. (2010) MMR gene expression pattern in sporadic colorectal cancer. *J Gastrointestin Liver Dis*, **19**, 155-159.
92. Dowen, J.M., Putnam, C.D. and Kolodner, R.D. (2010) Functional studies and homology modeling of Msh2-Msh3 predict that mispair recognition involves DNA bending and strand separation. *Mol Cell Biol*, **30**, 3321-3328.
93. Marra, G., Iaccarino, I., Lettieri, T., Roscilli, G., Delmastro, P. and Jiricny, J. (1998) Mismatch repair deficiency associated with overexpression of the MSH3 gene. *Proc Natl Acad Sci U S A*, **95**, 8568-8573.
94. Pegg, A.E. (1984) Methylation of the O6 position of guanine in DNA is the most likely initiating event in carcinogenesis by methylating agents. *Cancer Invest*, **2**, 223-231.
95. Vallen, E.A. and Cross, F.R. (1995) Mutations in RAD27 define a potential link between G1 cyclins and DNA replication. *Mol Cell Biol*, **15**, 4291-4302.
96. Reagan, M.S., Pittenger, C., Siede, W. and Friedberg, E.C. (1995) Characterization of a mutant strain of Saccharomyces cerevisiae with a deletion of the RAD27 gene, a structural homolog of the RAD2 nucleotide excision repair gene. *J Bacteriol*, **177**, 364-371.
97. Tishkoff, D.X., Boerger, A.L., Bertrand, P., Filosi, N., Gaida, G.M., Kane, M.F. and Kolodner, R.D. (1997) Identification and characterization of Saccharomyces cerevisiae EXO1, a gene encoding an exonuclease that interacts with MSH2. *Proc Natl Acad Sci U S A*, **94**, 7487-7492.
98. Becker, J.R., Pons, C., Nguyen, H.D., Costanzo, M., Boone, C., Myers, C.L. and Bielinsky, A.-K. (2015) Genetic Interactions Implicating Postreplicative Repair in Okazaki Fragment Processing. *PLOS Genetics*, **11**, e1005659.
99. Becker, J.R., Gallo, D., Leung, W., Croissant, T., Thu, Y.M., Nguyen, H.D., Starr, T.K., Brown, G.W. and Bielinsky, A.K. (2018) Flap endonuclease overexpression drives genome instability and DNA damage hypersensitivity in a PCNA-dependent manner. *Nucleic Acids Res*, **46**, 5634-5650.

100. Darzynkiewicz, Z., Zhao, H., Halicka, H.D., Rybak, P., Dobrucki, J. and Wlodkowic, D. (2012) DNA damage signaling assessed in individual cells in relation to the cell cycle phase and induction of apoptosis. *Crit Rev Clin Lab Sci*, **49**, 199-217.
101. Tanaka, S., Umemori, T., Hirai, K., Muramatsu, S., Kamimura, Y. and Araki, H. (2007) CDK-dependent phosphorylation of Sld2 and Sld3 initiates DNA replication in budding yeast. *Nature*, **445**, 328-332.
102. Huang, X., Halicka, H.D., Traganos, F., Tanaka, T., Kurose, A. and Darzynkiewicz, Z. (2005) Cytometric assessment of DNA damage in relation to cell cycle phase and apoptosis. *Cell Prolif*, **38**, 223-243.
103. Studamire, B., Price, G., Sugawara, N., Haber, J.E. and Alani, E. (1999) Separation-of-function mutations in Saccharomyces cerevisiae MSH2 that confer mismatch repair defects but do not affect nonhomologous-tail removal during recombination. *Mol Cell Biol*, **19**, 7558-7567.
104. Kadyrov, F.A., Dzantiev, L., Constantin, N. and Modrich, P. (2006) Endonucleolytic function of MutLalpha in human mismatch repair. *Cell*, **126**, 297-308.
105. Kadyrov, F.A., Holmes, S.F., Arana, M.E., Lukianova, O.A., O'Donnell, M., Kunkel, T.A. and Modrich, P. (2007) Saccharomyces cerevisiae MutLalpha is a mismatch repair endonuclease. *J Biol Chem*, **282**, 37181-37190.
106. Kadyrova, L.Y. and Kadyrov, F.A. (2016) Endonuclease activities of MutLα and its homologs in DNA mismatch repair. *DNA Repair (Amst)*, **38**, 42-49.
107. Smith, C.E., Mendillo, M.L., Bowen, N., Hombauer, H., Campbell, C.S., Desai, A., Putnam, C.D. and Kolodner, R.D. (2013) Dominant Mutations in S. cerevisiae PMS1 Identify the Mlh1-Pms1 Endonuclease Active Site and an Exonuclease 1-Independent Mismatch Repair Pathway. *PLOS Genetics*, **9**, e1003869.
108. Al-Sweel, N., Raghavan, V., Dutta, A., Ajith, V.P., Di Vietro, L., Khondakar, N., Manhart, C.M., Surtees, J.A., Nishant, K.T. and Alani, E. (2017) mlh3 mutations in baker's yeast alter meiotic recombination outcomes by increasing noncrossover events genome-wide. *PLoS Genet*, **13**, e1006974.
109. Young, S.J., Sebald, M., Shah Punatar, R., Larin, M., Masino, L., Rodrigo-Brenni, M.C., Liang, C.C. and West, S.C. (2020) MutSβ Stimulates Holliday Junction Resolution by the SMX Complex. *Cell Rep*, **33**, 108289.
110. Wilson, T., Guerrette, S. and Fishel, R. (1999) Dissociation of mismatch recognition and ATPase activity by hMSH2-hMSH3. *J Biol Chem*, **274**, 21659-21664.
111. Kulak, N.A., Pichler, G., Paron, I., Nagaraj, N. and Mann, M. (2014) Minimal, encapsulated proteomic-sample processing applied to copy-number estimation in eukaryotic cells. *Nature Methods*, **11**, 319-324.
112. Ghaemmaghami, S., Huh, W.K., Bower, K., Howson, R.W., Belle, A., Dephoure, N., O'Shea, E.K. and Weissman, J.S. (2003) Global analysis of protein expression in yeast. *Nature*, **425**, 737-741.
113. Arlow, T., Kim, J., Haye-Bertolozzi, J.E., Martínez, C.B., Fay, C., Zorensky, E., Rose, M.D. and Gammie, A.E. (2021) MutSα mismatch repair protein stability is governed by subunit interaction, acetylation, and ubiquitination. *G3 Genes|Genomes|Genetics*, **11**.
114. Kumar, C., Piacente, S.C., Sibert, J., Bukata, A.R., O'Connor, J., Alani, E. and Surtees, J.A. (2011) Multiple factors insulate Msh2-Msh6 mismatch repair activity from defects in Msh2 domain I. *J Mol Biol*, **411**, 765-780.

115. Chakraborty, U., Dinh, T.A. and Alani, E. (2018) Genomic Instability Promoted by Overexpression of Mismatch Repair Factors in Yeast: A Model for Understanding Cancer Progression. *Genetics*, **209**, 439-456.
116. Tomé, S., Simard, J.P., Slean, M.M., Holt, I., Morris, G.E., Wojciechowicz, K., te Riele, H. and Pearson, C.E. (2013) Tissue-specific mismatch repair protein expression: MSH3 is higher than MSH6 in multiple mouse tissues. *DNA Repair (Amst)*, **12**, 46-52.
117. Inokuchi, K., Ikejima, M., Watanabe, A., Nakajima, E., Orimo, H., Nomura, T. and Shimada, T. (1995) Loss of expression of the human MSH3 gene in hematological malignancies. *Biochem Biophys Res Commun*, **214**, 171-179.
118. Gomes-Pereira, M., Fortune, M.T., Ingram, L., McAbney, J.P. and Monckton, D.G. (2004) Pms2 is a genetic enhancer of trinucleotide CAG.CTG repeat somatic mosaicism: implications for the mechanism of triplet repeat expansion. *Hum Mol Genet*, **13**, 1815-1825.
119. Pinto, R.M., Dragileva, E., Kirby, A., Lloret, A., Lopez, E., St Claire, J., Panigrahi, G.B., Hou, C., Holloway, K., Gillis, T. *et al.* (2013) Mismatch repair genes Mlh1 and Mlh3 modify CAG instability in Huntington's disease mice: genome-wide and candidate approaches. *PLoS Genet*, **9**, e1003930.
120. Pluciennik, A., Burdett, V., Baitinger, C., Iyer, R.R., Shi, K. and Modrich, P. (2013) Extrahelical (CAG)/(CTG) triplet repeat elements support proliferating cell nuclear antigen loading and MutLα endonuclease activation. *Proc Natl Acad Sci U S A*, **110**, 12277-12282.
121. Miller, C.J., Kim, G.Y., Zhao, X. and Usdin, K. (2020) All three mammalian MutL complexes are required for repeat expansion in a mouse cell model of the Fragile X-related disorders. *PLoS Genet*, **16**, e1008902.
122. Roy, J.C.L., Vitalo, A., Andrew, M.A., Mota-Silva, E., Kovalenko, M., Burch, Z., Nhu, A.M., Cohen, P.E., Grabczyk, E., Wheeler, V.C. *et al.* (2021) Somatic CAG expansion in Huntington's disease is dependent on the MLH3 endonuclease domain, which can be excluded via splice redirection. *Nucleic Acids Res*, **49**, 3907-3918.
123. Casazza K, Williams GM, Johengen L, Lamb NA, Phelps S, Irwin B, Keller M, Twoey G and JA, S. (2022) All three MLH complexes contribute to promoting CAG and CTG trinucleotide repeat expansions in Saccharomyces cerevisiae. *biorxiv*.
124. Zhu, Q., Chang, Y., Yang, J. and Wei, Q. (2014) Post-translational modifications of proliferating cell nuclear antigen: A key signal integrator for DNA damage response (Review). *Oncol Lett*, **7**, 1363-1369.
125. Waters, L.S., Minesinger, B.K., Wiltrout, M.E., D'Souza, S., Woodruff, R.V. and Walker, G.C. (2009) Eukaryotic translesion polymerases and their roles and regulation in DNA damage tolerance. *Microbiol Mol Biol Rev*, **73**, 134-154.
126. Watanabe, K., Tateishi, S., Kawasuji, M., Tsurimoto, T., Inoue, H. and Yamaizumi, M. (2004) Rad18 guides poleta to replication stalling sites through physical interaction and PCNA monoubiquitination. *Embo j*, **23**, 3886-3896.
127. Hoege, C., Pfander, B., Moldovan, G.L., Pyrowolakis, G. and Jentsch, S. (2002) RAD6-dependent DNA repair is linked to modification of PCNA by ubiquitin and SUMO. *Nature*, **419**, 135-141.
128. Broomfield, S., Chow, B.L. and Xiao, W. (1998) MMS2, encoding a ubiquitin-conjugating-enzyme-like protein, is a member of the yeast error-free postreplication repair pathway. *Proceedings of the National Academy of Sciences*, **95**, 5678-5683.
129. Hofmann, R.M. and Pickart, C.M. (1999) Noncanonical MMS2-encoded ubiquitin-conjugating enzyme functions in assembly of novel polyubiquitin chains for DNA repair. *Cell*, **96**, 645-653.

130. Pâques, F. and Haber, J.E. (1999) Multiple pathways of recombination induced by double-strand breaks in Saccharomyces cerevisiae. *Microbiol Mol Biol Rev*, **63**, 349-404.
131. Parker, J.L., Bucceri, A., Davies, A.A., Heidrich, K., Windecker, H. and Ulrich, H.D. (2008) SUMO modification of PCNA is controlled by DNA. *Embo j*, **27**, 2422-2431.
132. Pfander, B., Moldovan, G.L., Sacher, M., Hoege, C. and Jentsch, S. (2005) SUMO-modified PCNA recruits Srs2 to prevent recombination during S phase. *Nature*, **436**, 428-433.
133. Papouli, E., Chen, S., Davies, A.A., Huttner, D., Krejci, L., Sung, P. and Ulrich, H.D. (2005) Crosstalk between SUMO and Ubiquitin on PCNA Is Mediated by Recruitment of the Helicase Srs2p. *Molecular Cell*, **19**, 123-133.
134. Parnas, O., Zipin-Roitman, A., Pfander, B., Liefshitz, B., Mazor, Y., Ben-Aroya, S., Jentsch, S. and Kupiec, M. (2010) Elg1, an alternative subunit of the RFC clamp loader, preferentially interacts with SUMOylated PCNA. *Embo j*, **29**, 2611-2622.
135. Kubota, T., Nishimura, K., Kanemaki, M.T. and Donaldson, A.D. (2013) The Elg1 replication factor C-like complex functions in PCNA unloading during DNA replication. *Mol Cell*, **50**, 273-280.
136. Kubota, T., Katou, Y., Nakato, R., Shirahige, K. and Donaldson, A.D. (2015) Replication-Coupled PCNA Unloading by the Elg1 Complex Occurs Genome-wide and Requires Okazaki Fragment Ligation. *Cell Rep*, **12**, 774-787.
137. Aroya, S.B. and Kupiec, M. (2005) The Elg1 replication factor C-like complex: a novel guardian of genome stability. *DNA Repair (Amst)*, **4**, 409-417.
138. McMurray, C.T. (2008) Hijacking of the mismatch repair system to cause CAG expansion and cell death in neurodegenerative disease. *DNA Repair (Amst)*, **7**, 1121-1134.
139. McMurray, C.T. (2010) Mechanisms of trinucleotide repeat instability during human development. *Nat Rev Genet*, **11**, 786-799.
140. Kadyrova, L.Y., Gujar, V., Burdett, V., Modrich, P.L. and Kadyrov, F.A. (2020) Human MutLγ, the MLH1-MLH3 heterodimer, is an endonuclease that promotes DNA expansion. *Proc Natl Acad Sci U S A*, **117**, 3535-3542.

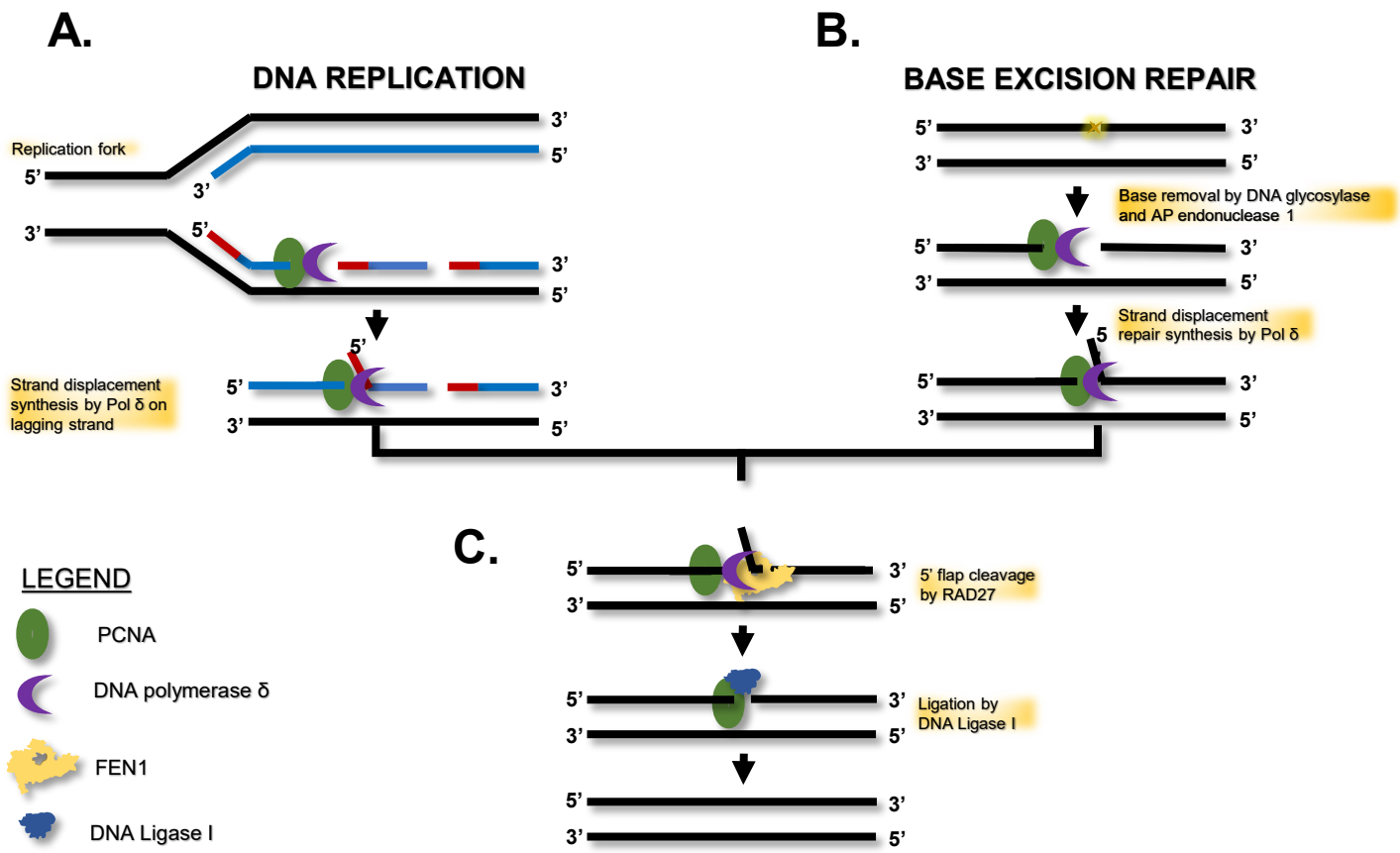

Figure 1. Two DNA metabolic pathways that involve 5' ssDNA flap processing

(A) During lagging strand synthesis DNA polymerase δ (Pol δ) initiates strand displacement synthesis when it encounters the upstream Okazaki fragment. (B) Base excision repair (BER) pathway is the primary mechanism to remove alkylation (and other) DNA damage. In long patch BER, DNA glycosylase catalyzes cleavage of the N-glycosidic bond of a damaged base to generate an apurinic/apyrimidinic (AP) site. AP endonuclease cleaves the AP site to generate a gap intermediate in which two or more (<10) nucleotides are removed. If polymerase δ is recruited for gap filling synthesis, this will lead to strand displacement. (C) In both pathways, a 5' ssDNA flap structure is formed. Rad27 binds and cleaves the flap and Cdc9 ligates the resulting nick, leading to either a continuous lagging strand or repaired DNA.

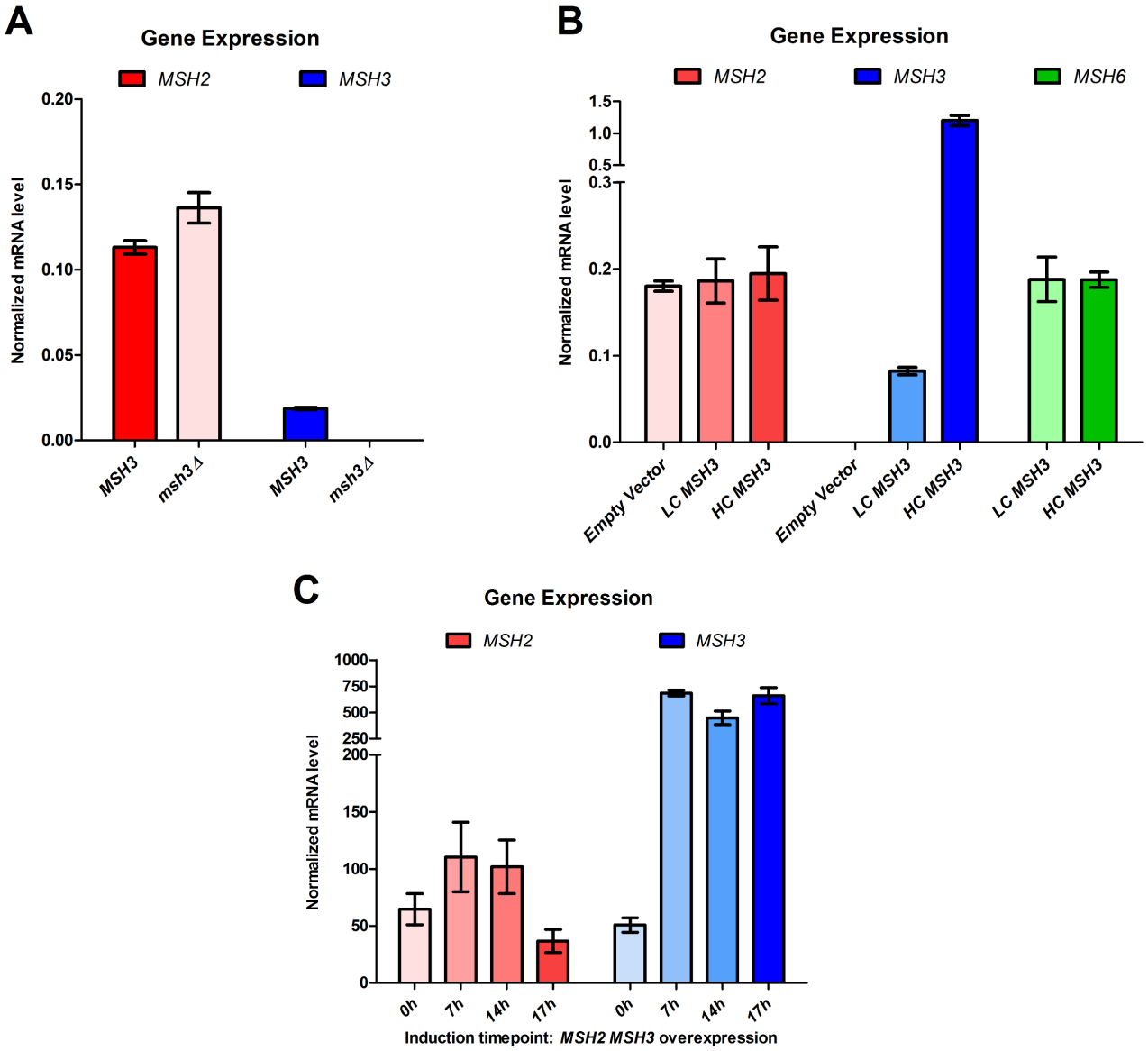

Figure. 2 Expression levels of *MSH2*, *MSH3* and *MSH6* in different cellular contexts. (**A**) RNA was isolated from *MSH3* or *msh3Δ* yeast cells at mid-log phase. Endogenous mRNA levels of *MSH2* (left panel, pink) and *MSH3* (right panel, blue) were determined by qRT-PCR. (**B**) RNA was isolated at mid-log phase from *msh3Δ* strains that carried an empty vector (pRS424), low copy (pSP18; *ARS CEN;* LC) or high copy (pSP15; *2μ; HC*) number plasmid bearing *MSH3* under the control of the endogenous *MSH3* promoter, respectively. mRNA expression levels of *MSH2* (pink), *MSH3* (blue), and *MSH6* (green) were determined by qRT-PCR. (**C**) qRT-PCR analysis of *MSH2* (pink) and *MSH3* (blue) co-overexpression mRNA levels in a *msh3Δ* background. Culture aliquots were collected at indicated hours after induction with galactose. RNA was extracted, and mRNA levels were quantified utilizing qRT-PCR. All RNA levels were normalized to the reference gene *PDA1.* Numbers represent the mean of at least three independent experiments. Error bars represent the standard error of the mean (SEM).

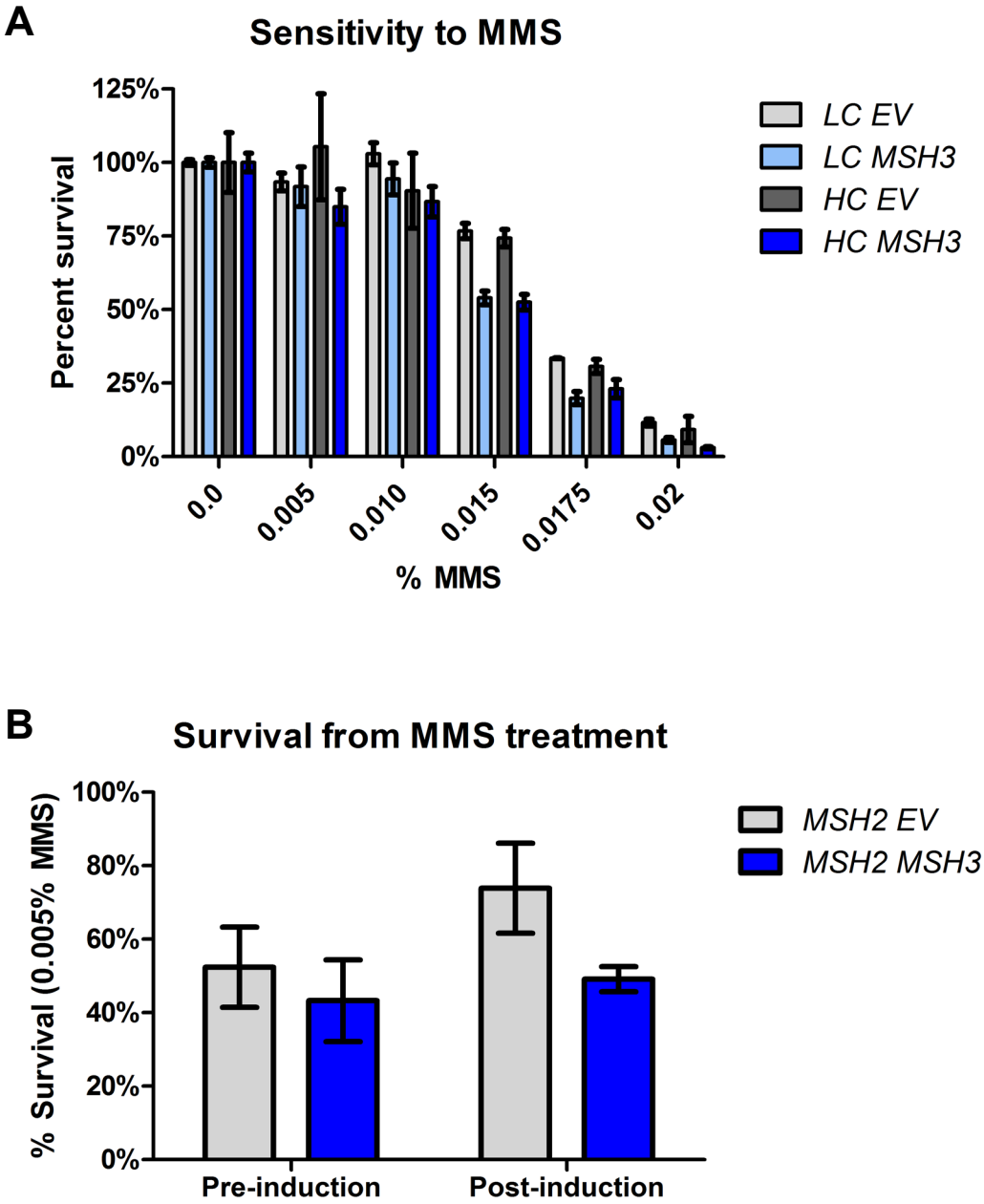

Figure 3. Elevated *MSH3* expression renders cells sensitive to methyl methanesulfonate (MMS). (**A**) MMS sensitivity of *msh3Δ* strains carrying either a low-copy (*LC*, light shade) or high-copy number (*HC*, dark shade) plasmid containing either empty vector (EV, gray bars) or *MSH3* (blue bars) were grown in increasing concentrations of MMS. Plotted graphs represent at least two independent experiments done in triplicate and with at least two independent transformants. Error bars were calculated by SEM. (**B**) MMS sensitivity of *msh3Δ* strains co-overexpressing *MSH2* and *MSH3*. Cultures were grown to mid-log phase and *MSH3* expression was induced by the addition of galactose. Time point 17 hours after induction was collected, serial diluted, and plated onto SC agar plates in the absence or presence of 0.005% MMS. Plotted data represents the results of at least three independent experiments. Error bars represent the SEM.

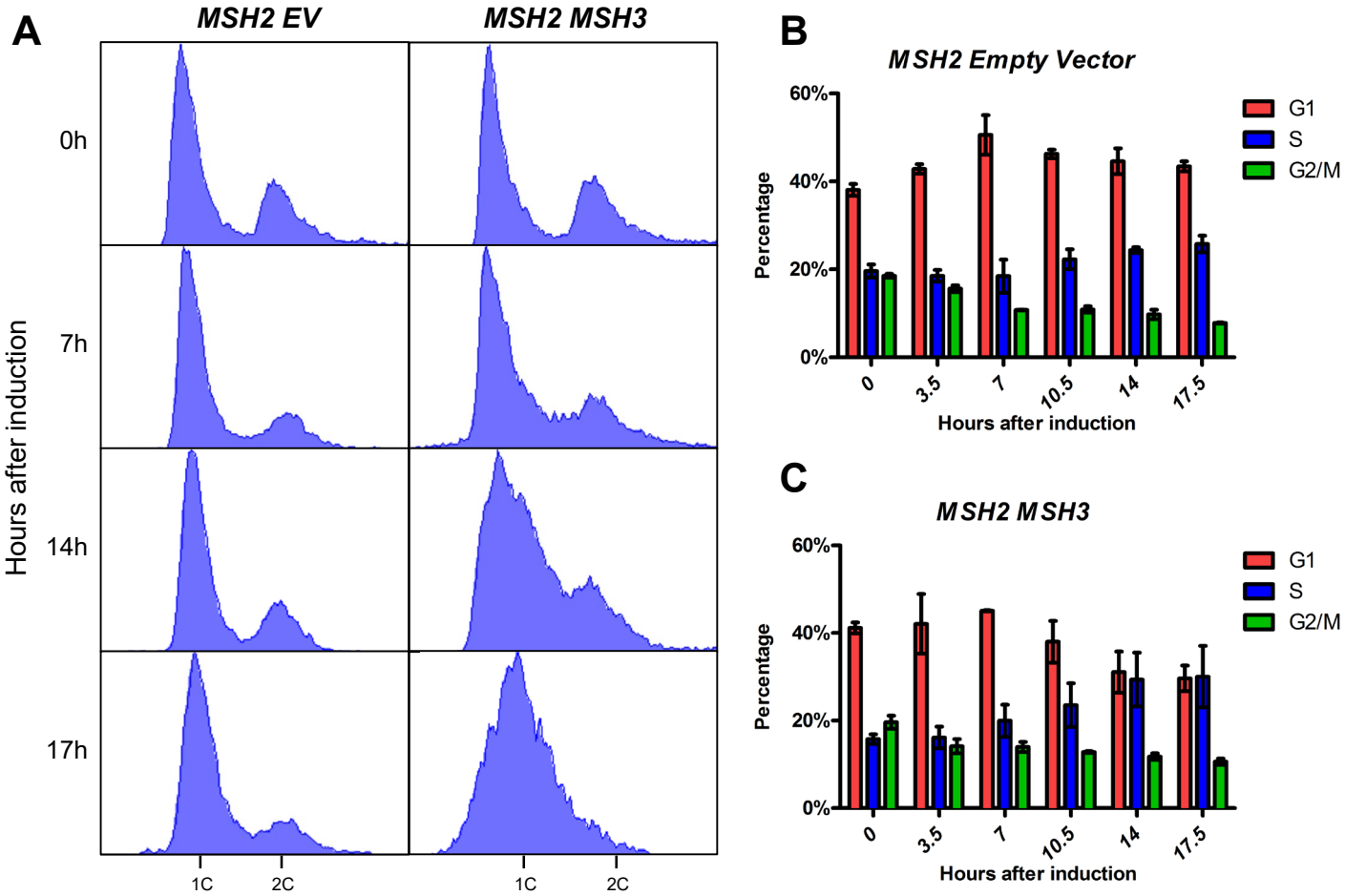

Figure 4. *MSH2-MSH3* overexpression induces a delay in cell cycle progression. *MSH2* and *MSH3* were overexpressed following galactose induction in a *msh3Δ* background. Aliquots were collected at indicated hours after induction. (A) Histograms are shown of chromosomal content of asynchronous populations of *MSH2 + empty vector (EV)* and *MSH2 + MSH3* at several timepoints following addition of galactose. Flow cytometry experiments were repeated at least three times, with at least two independent transformants. 1C indicates 1x DNA content; 2C indicates 2x DNA content. (B and C) Quantification of relative proportion of cells in different phases of the cell cycle for *MSH2 + EV* (B) or *MSH2 + MSH3* (C). The percentage of cells in G1 (1C), G2/M (2C) or S (between 1C and 2C) phases was determined using BD FACSDiva 8.0 software (see Figure S1 for details). Plotted values correspond to data collected from at least three independent experiments. Error bars represent SEM.

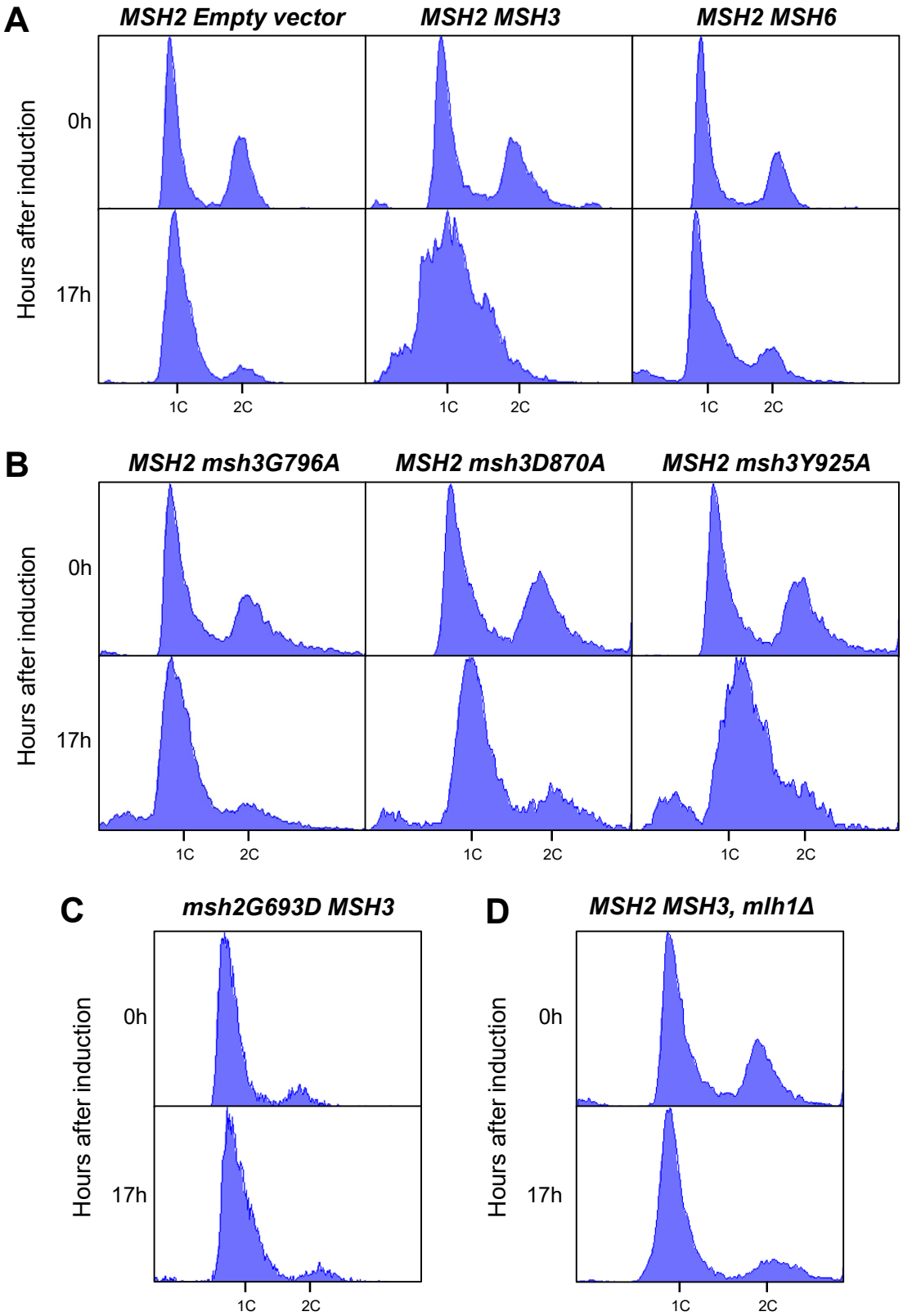

Figure 5. *MSH2 MSH3* overexpression-mediated cell cycle defects depends on *MSH3* ATP binding and hydrolysis function. *MSH2* **(A, B, D)** or *msh2G693D* **(C)** was co-overexpressed with empty vector (EV)*, MSH6, MSH3,* or *msh3* alleles in a *msh3Δ* **(A, B, C)** or *mlh1Δ* **(D)** background. *MSH2* was constitutively overexpressed; for all others, expression was induced with galactose. Aliquots were collected at 0 and 17 hours after induction. Harvested cells were fixed, stained, and processed by flow cytometry. Histograms of the asynchronous population are shown.

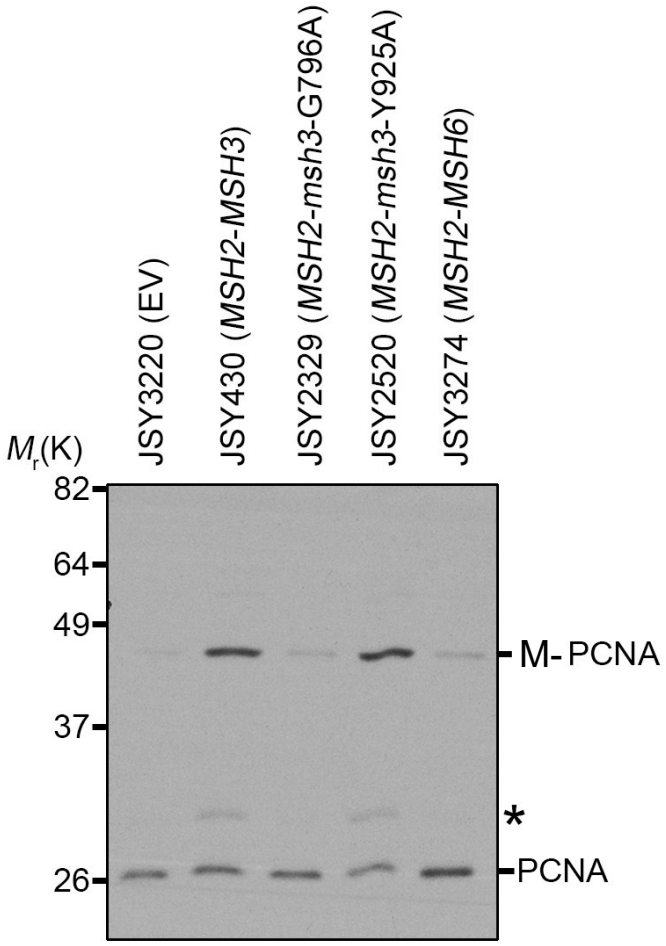

Figure 6. *MSH2 MSH3* overexpression induced PCNA modification that depends on ATP binding and hydrolysis. *MSH2* and *MSH3* or *msh3* alleles were overexpressed in a *msh3Δ* background, as previously described. Samples were taken following induction and TCA protein extracts were prepared and the proteins were separated by 10% SDS-PAGE, transferred into a membrane and then probed with anti-PCNA. Modified PCNA is marked as M-PCNA. The asterisk indicates non-specific bands.

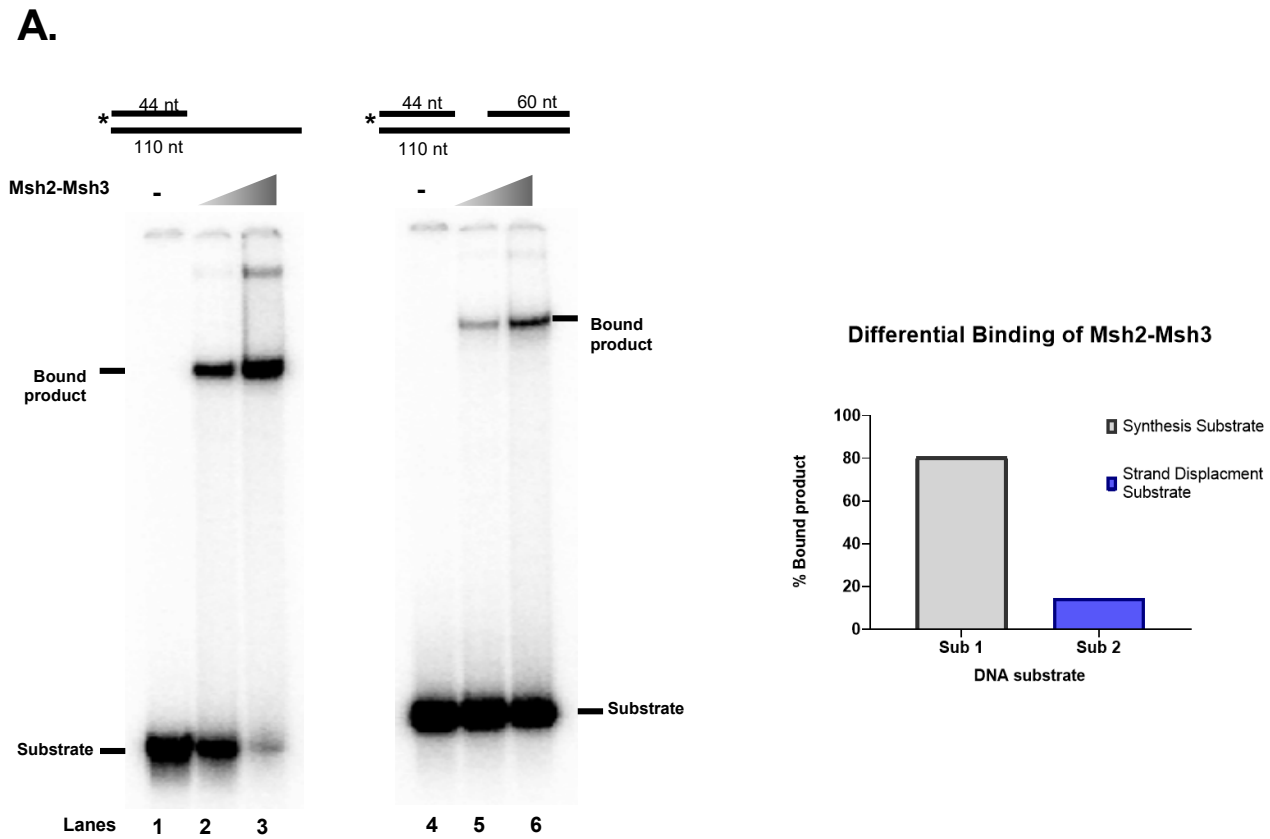

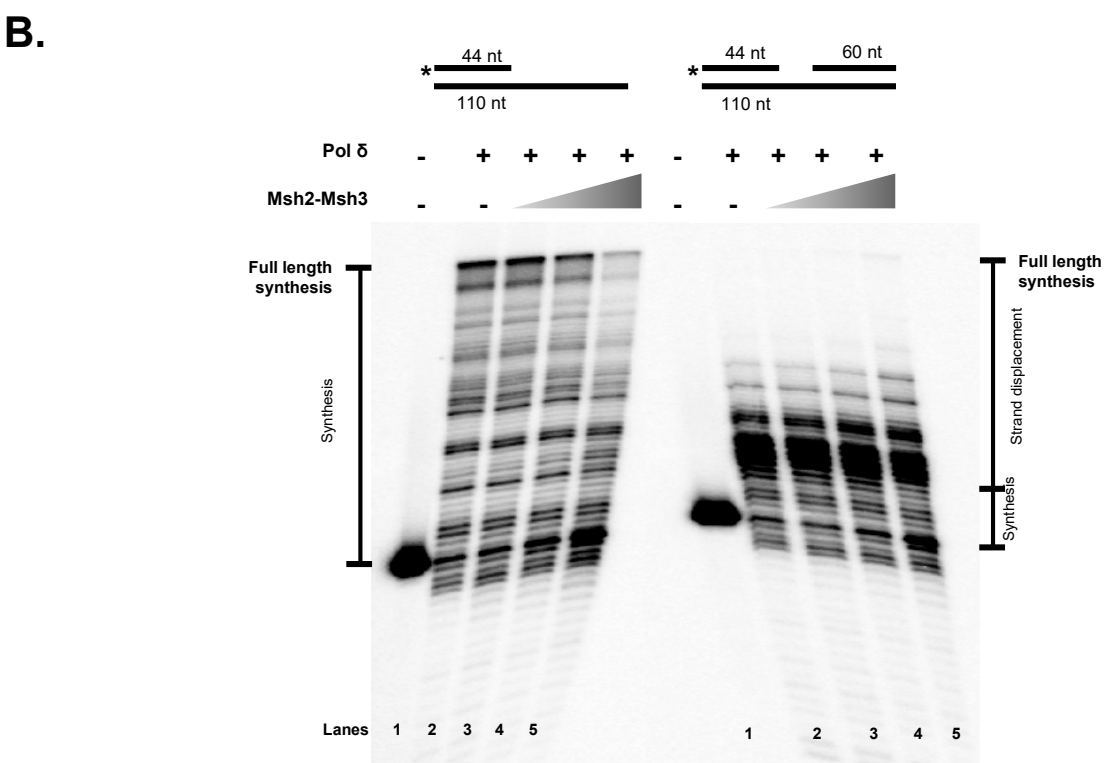

Figure 7. Msh2-Msh3 modulate DNA polymerase d activity in a DNA substrate-dependent manner. (**A**) Msh2-Msh3 binds to the synthesis substrate (left) and the strand displacement substrate (right) with different affinities. Quantification is shown in right panel. (**B**) Msh2-Msh3 inhibits DNA polymerase d in the presence of synthesis substrate (left) and stimulates its strand displacement synthesis activity (right).